

Supporting information for:

UNDERSTANDING THE ROLE OF TYROSINE IN GLYCOGENIN

Ander Camiruaga,^{a†} Imanol Usabiaga,^a Aran Insausti,^a Emilio J. Cocinero,^a Iker León,^{ab} and José A. Fernández^{a*}*

^aDep. of Physical Chemistry, Fac. of Science and Technology, University of the Basque Country (UPV/EHU), Barrio Sarriena, s/n, 48940 Leioa, Spain

^bCurrent address: Grupo de Espectroscopía Molecular (GEM), Edificio Quifima, Laboratorios de Espectroscopia y Bioespectroscopia, Unidad Asociada CSIC, Parque Científico UVA, Universidad de Valladolid, 47011 Valladolid, Spain

*Corresponding Authors:

Iker León, iker.leon@ehu.es

José A. Fernández, josea.fernandez@ehu.es

phone: +34946015387

fax: +34946013500

web: <https://sites.google.com/site/gesemupv/>

† A. Camiruaga and I. Usabiaga contributed equally to this work.

Theoretical methods. A critical aspect of this study was to ensure that the conformational landscape was thoroughly explored, as small, experimentally non-significant changes in the relative orientation of some chemical groups may result in shifts in the IR bands that may derive in incorrect assignments of the experimental spectra. Therefore, to ensure that no important structures were left out, the same computational procedure already tested successfully for similar systems was used.¹⁻⁴ It consists of three stages. First, an automated exploration of the intermolecular potential energy surface was carried out using fast molecular mechanics methods (MMFFs) and two search algorithms: the “Large scales Low Mode” (which uses frequency modes to create new structures) and a Monte Carlo-based search, as implemented in Macromodel (www.schrodinger.com). In a second stage, the structures were inspected using chemical intuition, looking for alternatives which implicate small rotations or changes in the relative position of functional groups. In this way, a large number of structures were obtained, some of them differing in subtle changes that posed no chemical meaning. Therefore, to compact them into a more manageable number without losing information, they were passed to a clustering algorithm that grouped them into families. Representative structures of each family were then chosen to be subjected to full optimization at the M06-2x/6-311++G(d,p) calculation level as implemented in Gaussian 09,⁵ which has proven to yield accurate results for similar systems. A normal mode analysis highlighted the validity of the optimized structures as true minima and allowed us to compute the zero point energy (ZPE). Thus, the energy values given in this work include the ZPE correction. The basis set superposition error was also estimated using the counterpoise procedure of Boys and Bernard.⁶

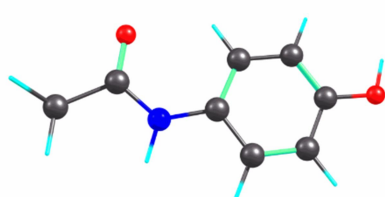
Finally, the entropy and the Gibbs free energy was calculated for each optimized structure in the 0-700 K interval using the output from the Gaussian calculations and the tools supplied by the NIST (http://www.nist.gov/mml/csd/informatics_research/thermochemistry_script.cfm). A detailed explanation of the procedure can be found in ref 1.

Experimental methods. The experimental system was described in detail in ref 1 and consists of a modified time of flight mass spectrometer equipped with a laser desorption/ionization (LDI) source attached to a pulsed valve (Series 9, General Valve Inc.), a Nd/YAG-pumped dye laser (Fine Adjustment Pulsare Pro-S), an OPO system (LaserVision) to generate light in the IR region and electronics for synchronization and data collection and handling. Ar was used as a carrier gas at a backing pressure of 10 bar.

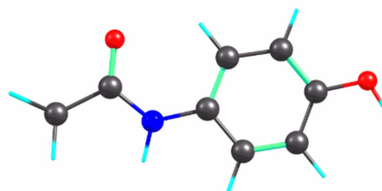
Preparation of the sample was done using a similar procedure to that explained in ref 1 and herein.

For the one color REMPI experiments the desorption laser was fired $\sim 207 \mu\text{s}$ after the valve opening, so the sample was picked by the jet. Approximately $200 \mu\text{s}$ later the UV laser was scanned while the final population of molecules at a given mass channel was recorded. For the IR experiments, similarly the desorption laser was fired $\sim 207 \mu\text{s}$ after the valve opening, so the sample was picked by the jet. Approximately $200 \mu\text{s}$ later the depopulation IR was fired and the final population of molecules was probed by a UV laser fired 50 ns later. A webcam inside the vacuum chamber allowed us to optimize the alignment of the ablation laser and to monitor the sample at any moment, enhancing the overall performance of the experimental set up.

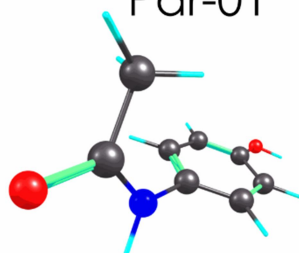
Figure S01. Calculated structures for Paracetamol (par), β -MeGlc and β -PhGlc monomers at M06-2X/6-311++G(d,p) level arranged in energetically order respect to the global minimum.



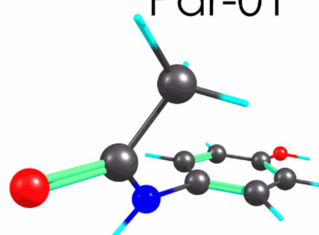
Par-01



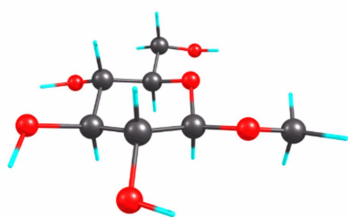
Par-01



Par-03



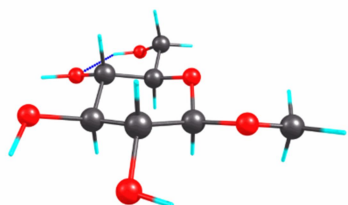
Par-04



β -MeGlc-01



β -MeGlc-02



β -MeGlc-03

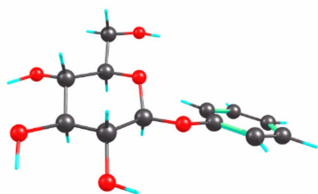


β -MeGlc-04



β -MeGlc-05

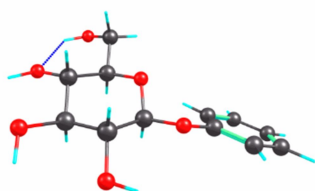
Figure S01. Cont.



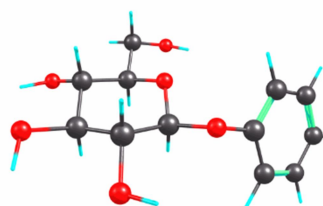
β -PhGlc-01



β -PhGlc-02



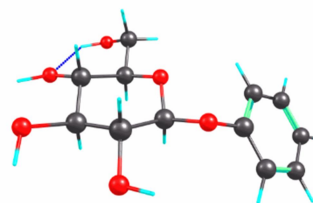
β -PhGlc-03



β -PhGlc-04



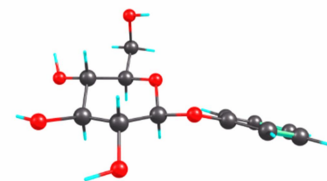
β -PhGlc-05



β -PhGlc-06



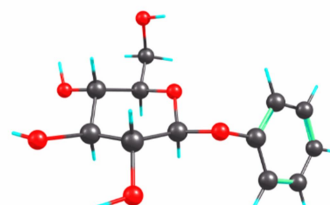
β -PhGlc-07



β -PhGlc-08



β -PhGlc-09



β -PhGlc-10

Table S01. Energies, ZPE, BSSE, thermal corrections, relative energies and thermal free energies at 298.15 K (ΔG) calculated at M-062X/6-311++G(d,p) level for the Paracetamol (par), β -MeGlc and β -PhGlc monomers.

Structure	Energy (Hartree)	ZPE (Hartree)	Thermal Correction (Hartree)	Relative Energy (kJ/mol)	Relative Gibbs Free Energy (kJ/mol)
β -MeGlc-2	-726.435571	0.229235	0.189588	0.00	0.00
β -MeGlc-1	-726.434974	0.228913	0.189537	0.72	1.43
β -MeGlc-3	-726.435015	0.229374	0.190386	1.82	3.55
β -MeGlc-5	-726.430868	0.229148	0.18958	12.12	12.33
β -MeGlc-4	-726.428038	0.22886	0.189193	18.79	18.74

Structure	Energy (Hartree)	ZPE (Hartree)	Thermal Correction (Hartree)	Relative Energy (kJ/mol)	Relative Gibbs Free Energy (kJ/mol)
β -PhGlc-1	-918.148769	0.281637	0.237167	0.00	0.00
β -PhGlc-2	-918.148303	0.281844	0.237559	1.77	2.25
β -PhGlc-3	-918.147723	0.282161	0.238269	4.12	5.64
β -PhGlc-5	-918.146287	0.281640	0.236675	6.52	5.22
β -PhGlc-4	-918.146551	0.281975	0.237231	6.71	5.99
β -PhGlc-6	-918.145782	0.281954	0.237133	8.67	7.75
β -PhGlc-8	-918.144428	0.281832	0.237328	11.91	11.82
β -PhGlc-7	-918.142671	0.281169	0.236572	14.78	14.45
β -PhGlc-10	-918.142498	0.281676	0.235892	16.57	13.12
β -PhGlc-9	-918.140614	0.281679	0.236713	21.52	20.22

Structure	Energy (Hartree)	ZPE (Hartree)	Thermal Correction (Hartree)	Relative Energy (kJ/mol)	Relative Gibbs Free Energy (kJ/mol)
Par-01	-515.651595	0.158361	0.121017	0	0
Par-02	-515.650948	0.158296	0.120901	1.528041	1.3941405
Par-03	-515.648601	0.158363	0.121519	7.865998	9.178748
Par-04	-515.648618	0.158398	0.121557	7.913257	9.2338835

Figure S02. Calculated structures for β -MeGlc•Par at M06-2X/6-311++G(d,p) level arranged in energetically order respect to the global minimum.

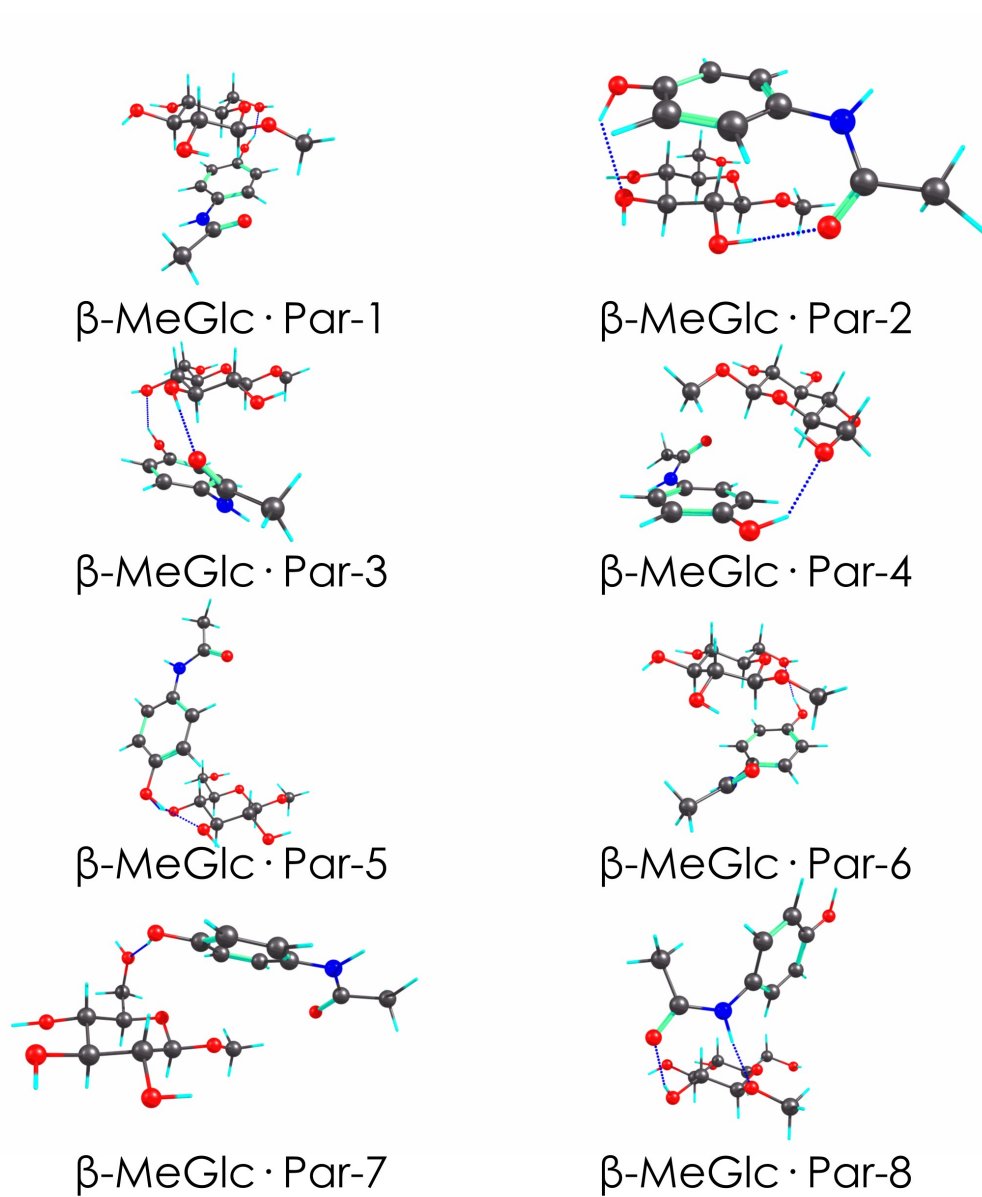
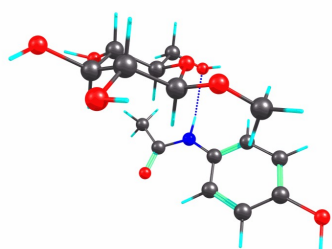
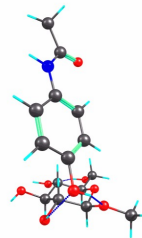


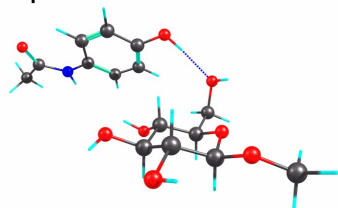
Figure S02. Cont.



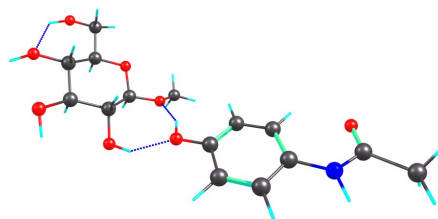
β -MeGlc · Par-9



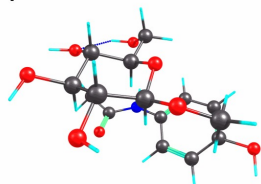
β -MeGlc · Par-10



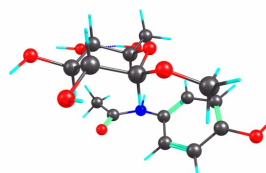
β -MeGlc · Par-11



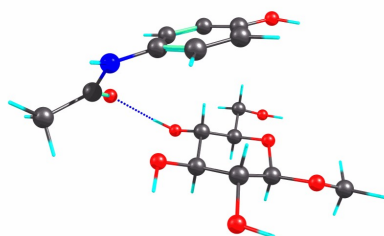
β -MeGlc · Par-12



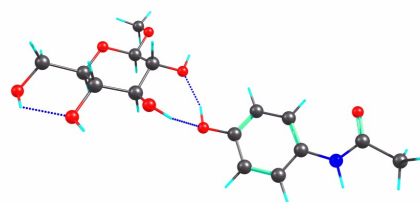
β -MeGlc · Par-13



β -MeGlc · Par-14

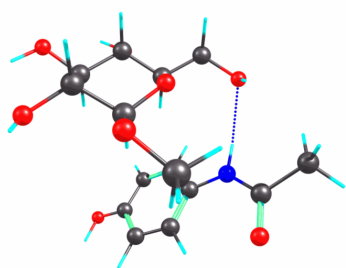


β -MeGlc · Par-15

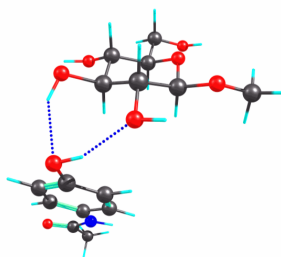


β -MeGlc · Par-16

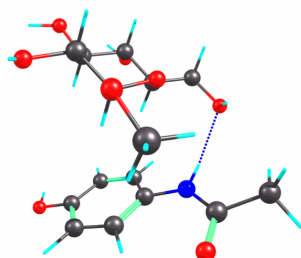
Figure S02. Cont.



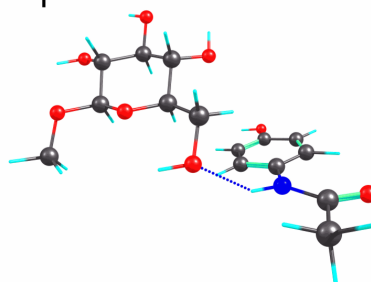
β -MeGlc · Par-17



β -MeGlc · Par-18



β -MeGlc · Par-19

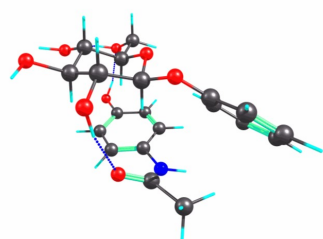


β -MeGlc · Par-20

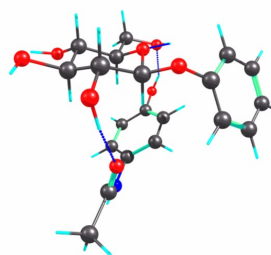
Table S02. Energies, ZPE, BSSE, thermal corrections, relative energies, thermal free energies at 298.15 K (ΔG) and the equilibrium temperature calculated at M-062X/6-311++G(d,p) level for the β -MeGlc•Par conformers.

Structure	Energy (Hartree)	ZPE (Hartree)	BSSE (Hartree)	Thermal Correction (Hartree)	Relative Energy (kJ/mol)	Relative Gibbs Free Energy (kJ/mol)	Equilibrium Temperature (K)
β -MeGlc · Par-01	-1241.881367	0.392018	0.0041125	0.338233	0.00	0.00	248.7
β -MeGlc · Par-02	-1241.87936	0.391552	0.0041215	0.336806	4.07	1.52	238.6
β -MeGlc · Par-03	-1241.88017	0.392291	0.0041192	0.337883	3.88	2.22	236.3
β -MeGlc · Par-04	-1241.877276	0.391846	0.0029958	0.335485	7.36	3.53	238.8
β -MeGlc · Par-05	-1241.875143	0.392	0.0025493	0.333503	12.19	3.92	236.3
β -MeGlc · Par-06	-1241.878919	0.391398	0.0039415	0.338122	4.35	6.14	224.7
β -MeGlc · Par-07	-1241.876618	0.391339	0.0040004	0.335932	10.39	6.43	212.0
β -MeGlc · Par-08	-1241.875676	0.391628	0.0026516	0.335155	10.08	6.86	224.9
β -MeGlc · Par-09	-1241.876301	0.391737	0.0029544	0.335999	9.52	7.44	220.1
β -MeGlc · Par-10	-1241.875134	0.392695	0.0026816	0.335031	14.39	7.96	213.7
β -MeGlc · Par-11	-1241.872699	0.391573	0.00265	0.333001	17.75	9.02	201.5
β -MeGlc · Par-12	-1241.872376	0.391791	0.0016091	0.332694	16.44	9.06	216.6
β -MeGlc · Par-13	-1241.876616	0.39202	0.0033915	0.337476	10.59	10.49	203.5
β -MeGlc · Par-14	-1241.8768	0.392162	0.0034542	0.337763	10.64	10.76	201.9
β -MeGlc · Par-15	-1241.875657	0.391788	0.0037639	0.336829	13.47	11.31	191.8
β -MeGlc · Par-16	-1241.873145	0.392644	0.0018091	0.33478	17.18	12.52	199.4
β -MeGlc · Par-17	-1241.875213	0.391974	0.0028808	0.337	12.81	12.92	195.6
β -MeGlc · Par-18	-1241.874394	0.391875	0.0025376	0.336498	13.80	13.75	197.0
β -MeGlc · Par-19	-1241.874735	0.391962	0.0028805	0.336956	14.03	14.06	189.6
β -MeGlc · Par-20	-1241.86836	0.391565	0.0016095	0.333101	26.39	20.68	146.6

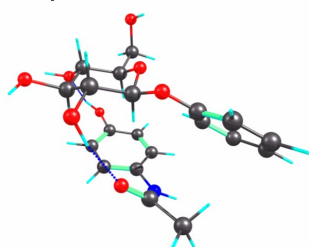
Figure S03. Calculated structures for β -PhGlc•Par at M06-2X/6-311++G(d,p) level arranged in energetically order respect to the global minimum.



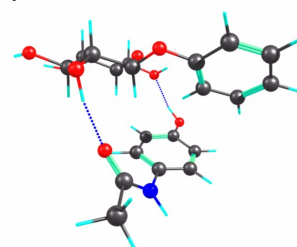
β -PhGlc • Par-01



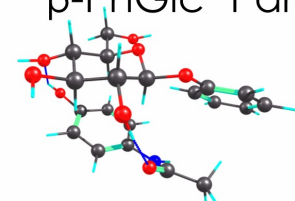
β -PhGlc • Par-02



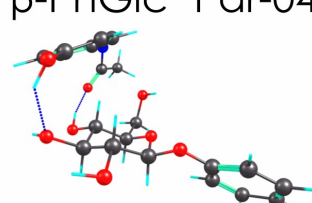
β -PhGlc • Par-03



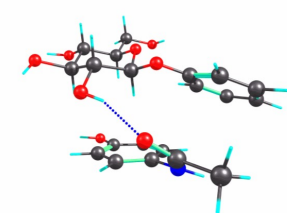
β -PhGlc • Par-04



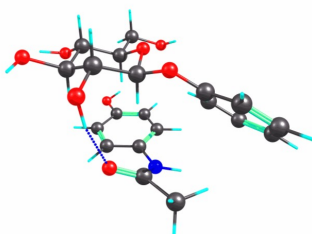
β -PhGlc • Par-05



β -PhGlc • Par-06

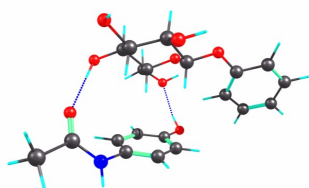


β -PhGlc • Par-07

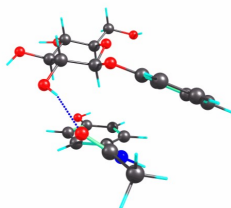


β -PhGlc • Par-08

Figure S03. Cont.



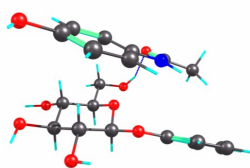
β -PhGlc · Par-09



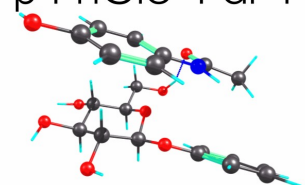
β -PhGlc · Par-10



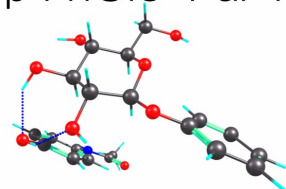
β -PhGlc · Par-11



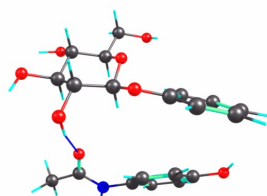
β -PhGlc · Par-12



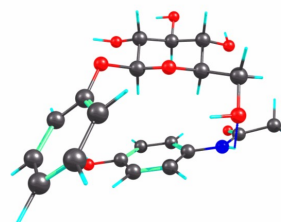
β -PhGlc · Par-13



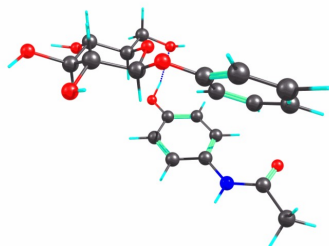
β -PhGlc · Par-14



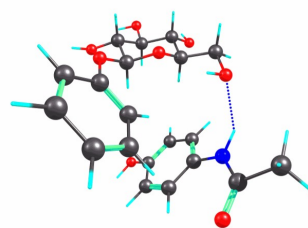
β -PhGlc · Par-15



β -PhGlc · Par-16



β -PhGlc · Par-17



β -PhGlc · Par-18

Table S03. Energies, ZPE, BSSE, thermal corrections, relative energies, thermal free energies at 298.15 K (ΔG) and the equilibrium temperature calculated at M-062X/6-311++G(d,p) level for the β -PhGlc•Par conformers.

Structure	Energy (Hartree)	ZPE (Hartree)	BSSE (Hartree)	Thermal Correction (Hartree)	Relative Energy (kJ/mol)	Relative Gibbs Free Energy (kJ/mol)	Equilibrium Temperature (K)
β -PhGlc • Par-01	-1433.602988	0.446332	0.0050614	0.390157	0.00	0.00	225.6
β -PhGlc • Par-02	-1433.598485	0.445039	0.0036299	0.385915	4.67	0.69	232.0
β -PhGlc • Par-03	-1433.599667	0.445002	0.0046896	0.387681	4.25	2.22	298.6
β -PhGlc • Par-04	-1433.597588	0.444972	0.0039585	0.385672	7.71	2.40	292.2
β -PhGlc • Par-05	-1433.600913	0.445466	0.0050857	0.389296	3.24	3.19	231.3
β -PhGlc • Par-06	-1433.598411	0.445087	0.0045369	0.387414	7.37	4.82	262.8
β -PhGlc • Par-07	-1433.596642	0.444421	0.0046471	0.386252	10.56	6.41	216.6
β -PhGlc • Par-08	-1433.597204	0.444815	0.0048203	0.386988	10.57	6.87	268.3
β -PhGlc • Par-09	-1433.595907	0.444799	0.0041636	0.385698	12.21	6.88	281.5
β -PhGlc • Par-10	-1433.596202	0.444723	0.0045836	0.386989	12.34	9.50	252.3
β -PhGlc • Par-11	-1433.593718	0.444896	0.0043555	0.384971	18.71	10.72	268.1
β -PhGlc • Par-12	-1433.595832	0.444449	0.0050616	0.387363	13.95	11.45	234.7
β -PhGlc • Par-13	-1433.59726	0.445584	0.0050748	0.389575	13.11	13.51	235.0
β -PhGlc • Par-14	-1433.589171	0.445051	0.0026784	0.382369	26.66	15.83	343.8
β -PhGlc • Par-15	-1433.591426	0.44467	0.0031556	0.384723	20.99	16.09	291.6
β -PhGlc • Par-16	-1433.591266	0.444317	0.0041786	0.384735	23.17	16.54	270.1
β -PhGlc • Par-17	-1433.592207	0.444673	0.003446	0.386167	19.71	17.83	232.0
β -PhGlc • Par-18	-1433.589867	0.444404	0.0028756	0.383944	23.65	18.14	224.6

Figure S04. IR spectra of β -MeGlc•Par and the predicted spectra for the structures in Figure S02 calculated at M06-2X/6-311++G(d,p). A correction factor of 0.932 was employed to account for the anharmonicity.

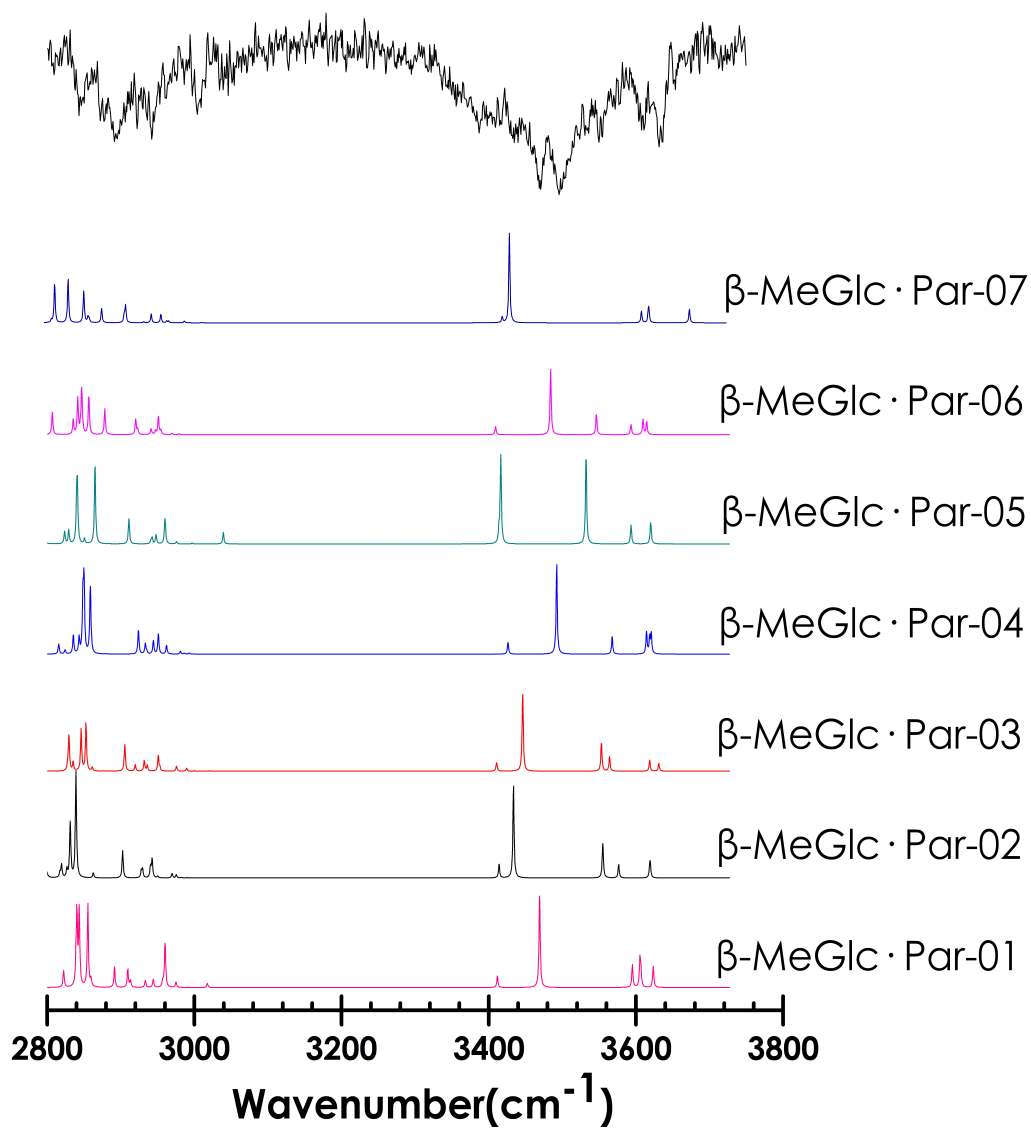


Figure S04. Cont.

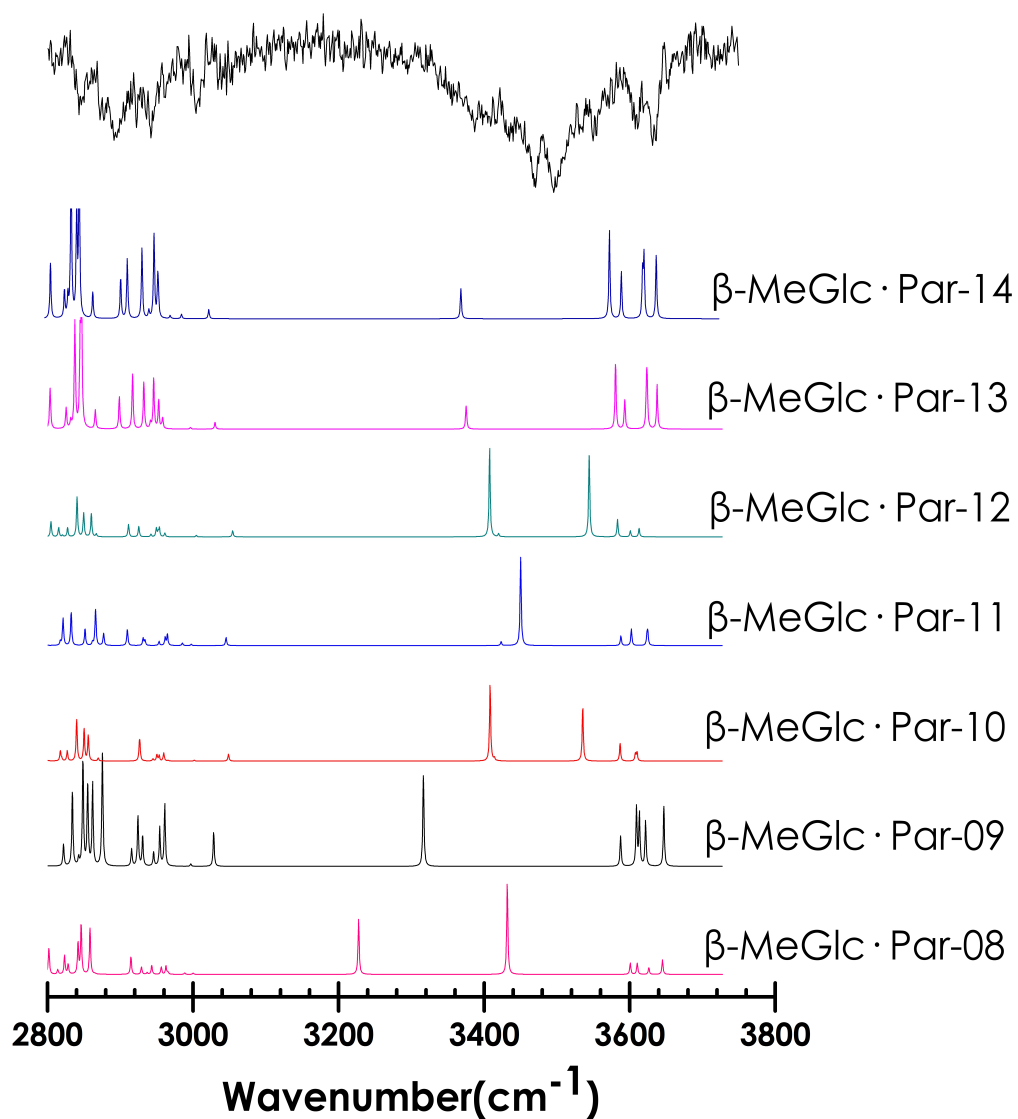


Figure S04. Cont.

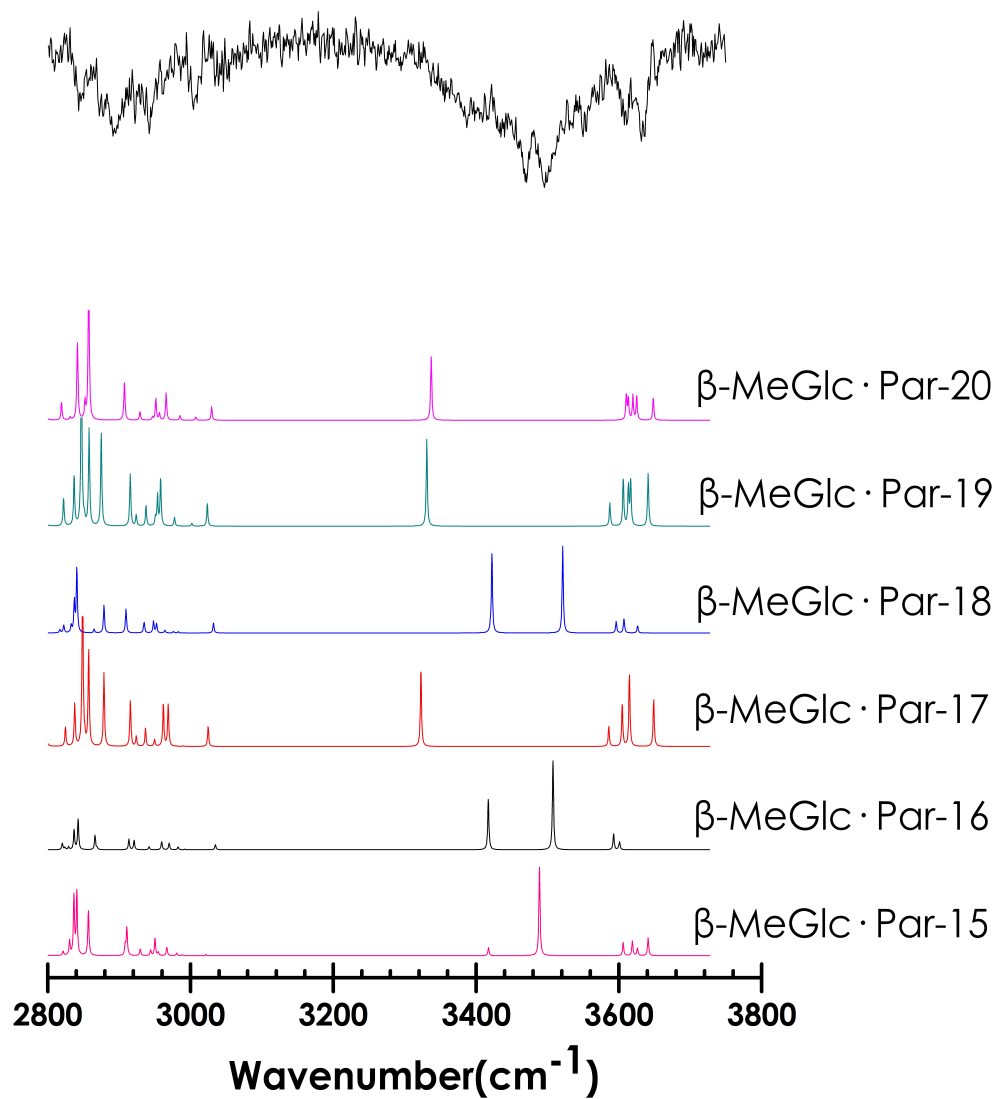


Figure S05. IR spectra of β -PhGlc•Par and the predicted spectra for the structures in Figure S03 calculated at M06-2X/6-311++G(d,p). A correction factor of 0.932 was employed to account for the anharmonicity.

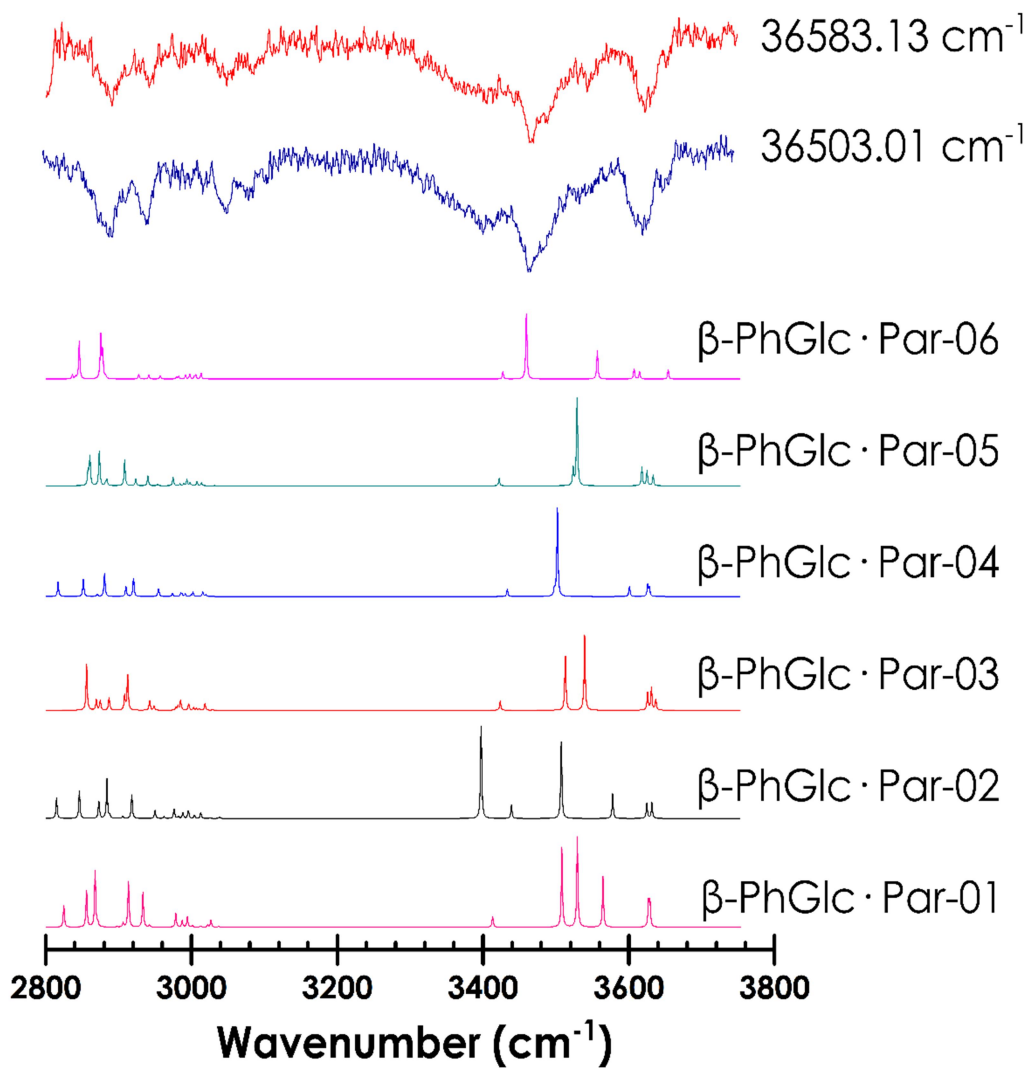


Figure S05. Cont.

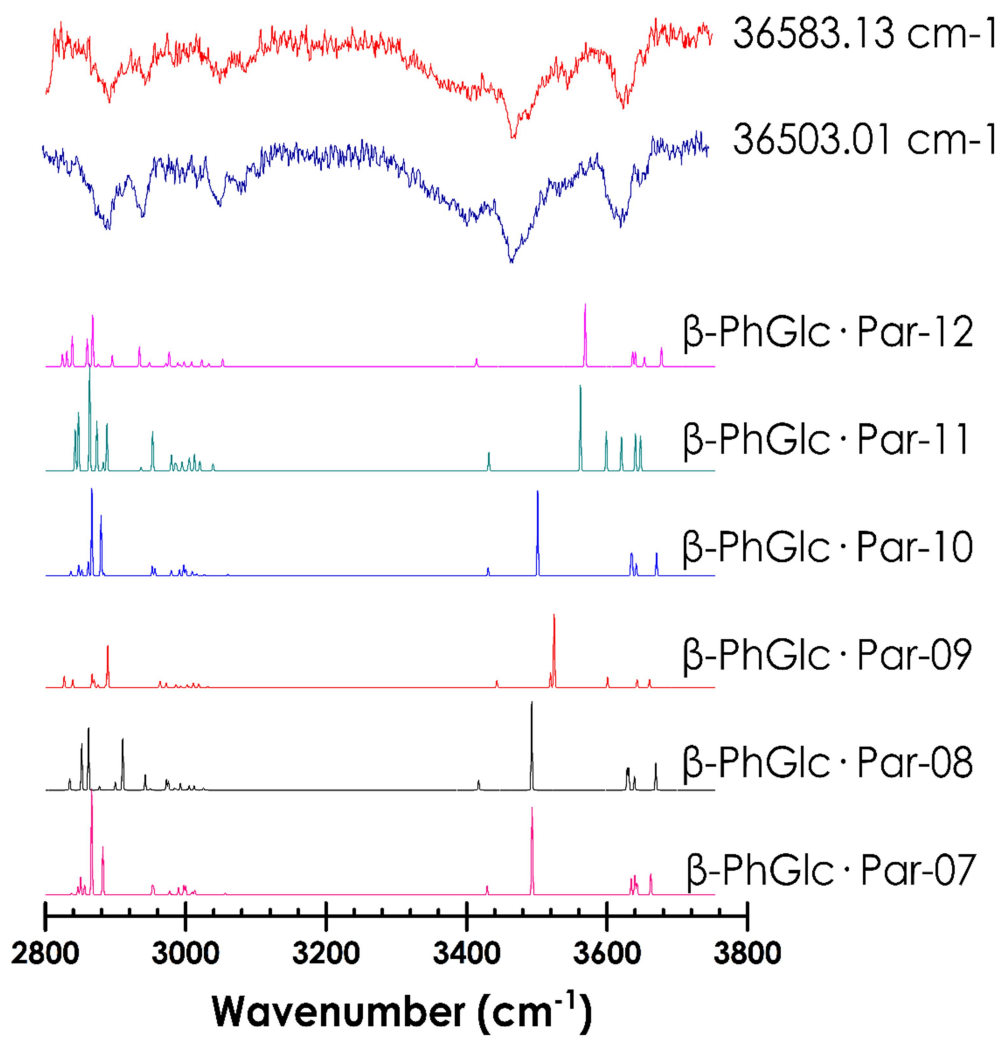


Figure S05. Cont.

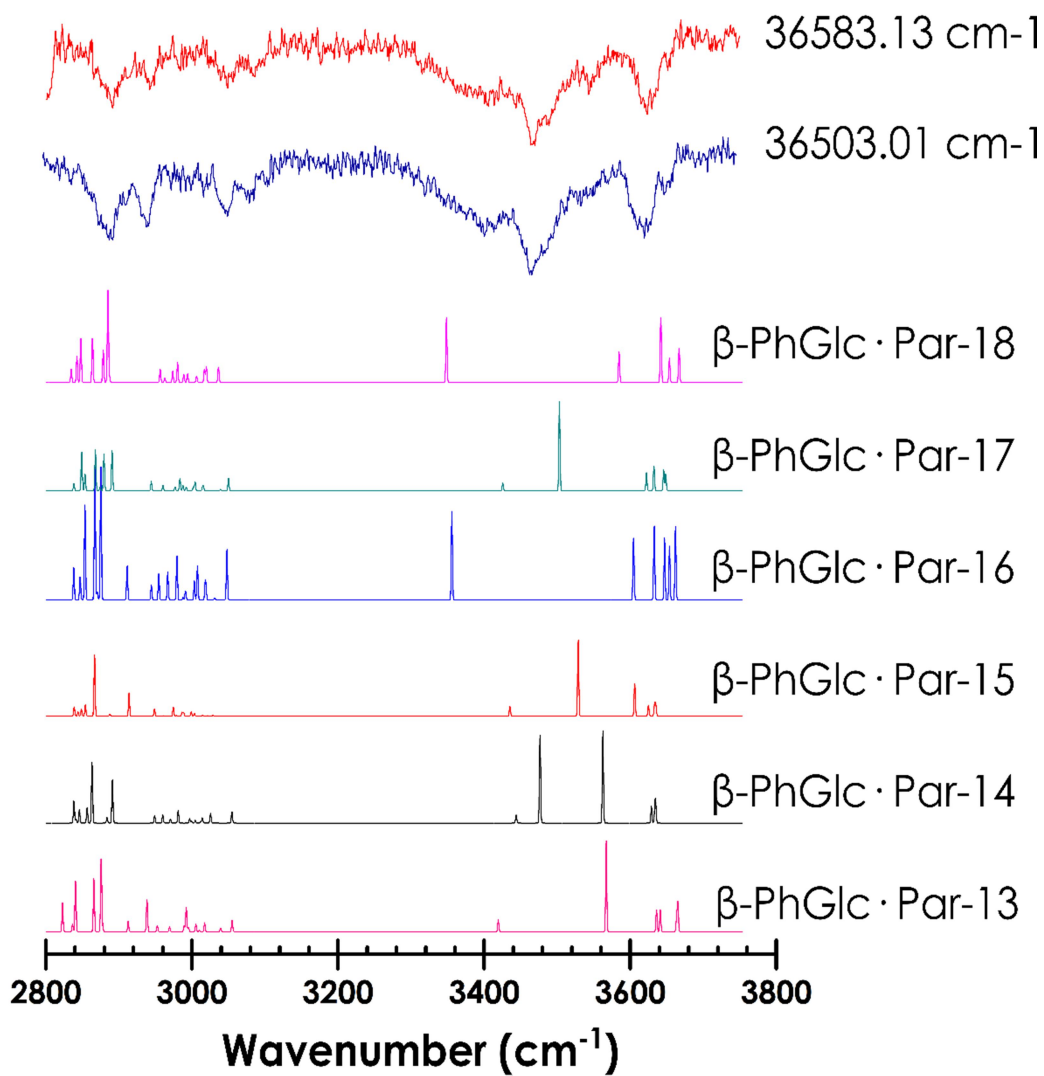
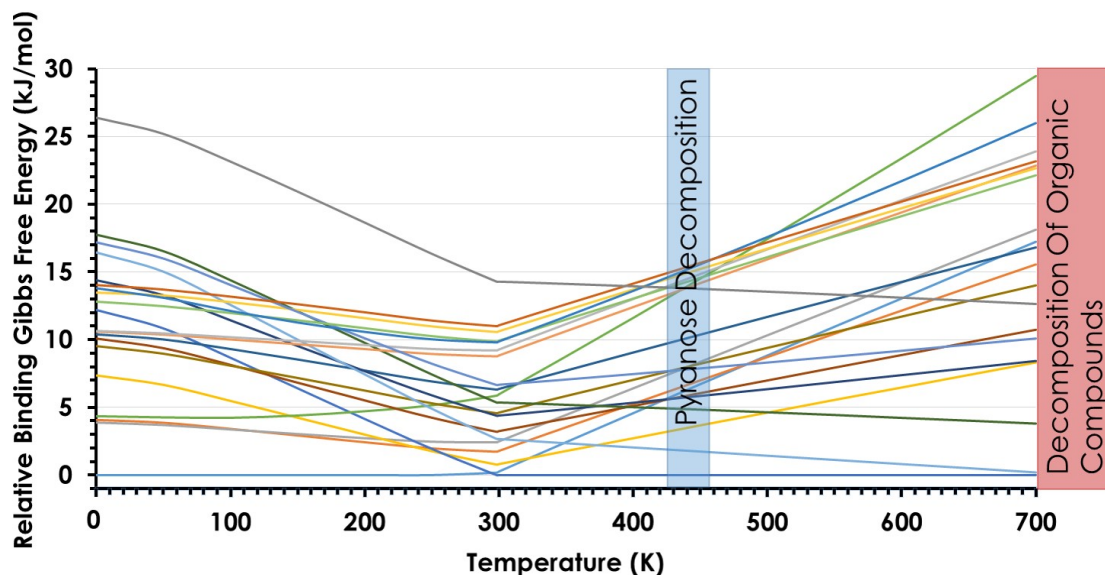


Figure S06. Gibbs relative free energy of the conformations for of β -MeGlc•Par for the structures in Figure S02. The red bar indicates the temperature at which most of the organic compounds decompose, while the blue bar indicates the temperature of decomposition of pyranose. The orange bar indicates where ΔG becomes positive and therefore, the cluster is no longer stable.



Structure of β -MeGlc • Par:
 1 — 2 — 3 — 4 — 5 — 6 — 7 — 8 — 9 — 10
 11 — 12 — 13 — 14 — 15 — 16 — 17 — 18 — 19 — 20

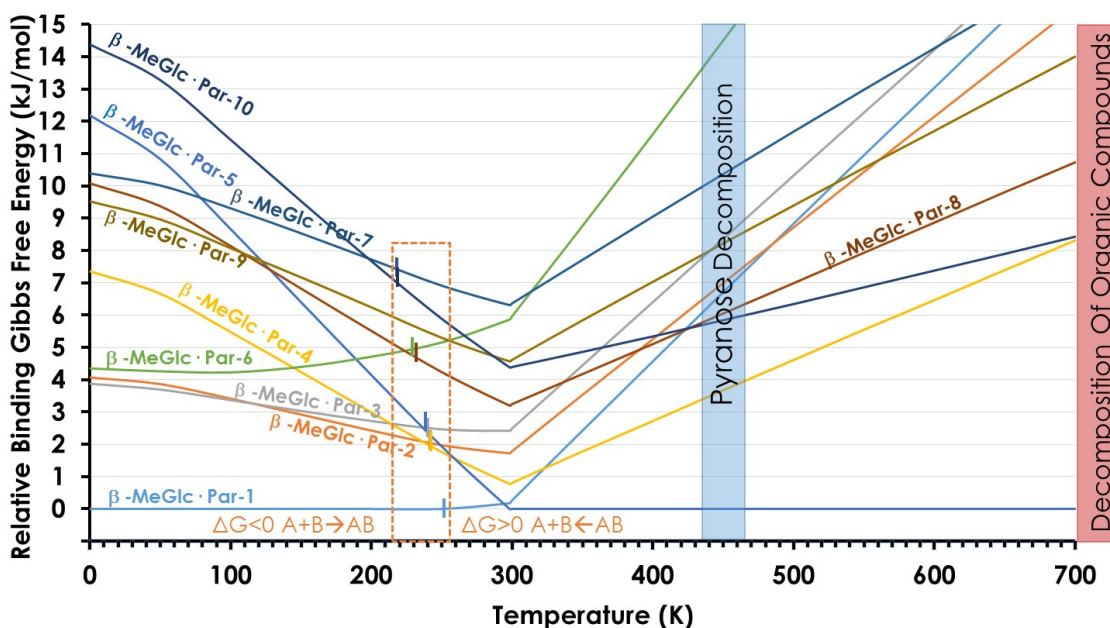
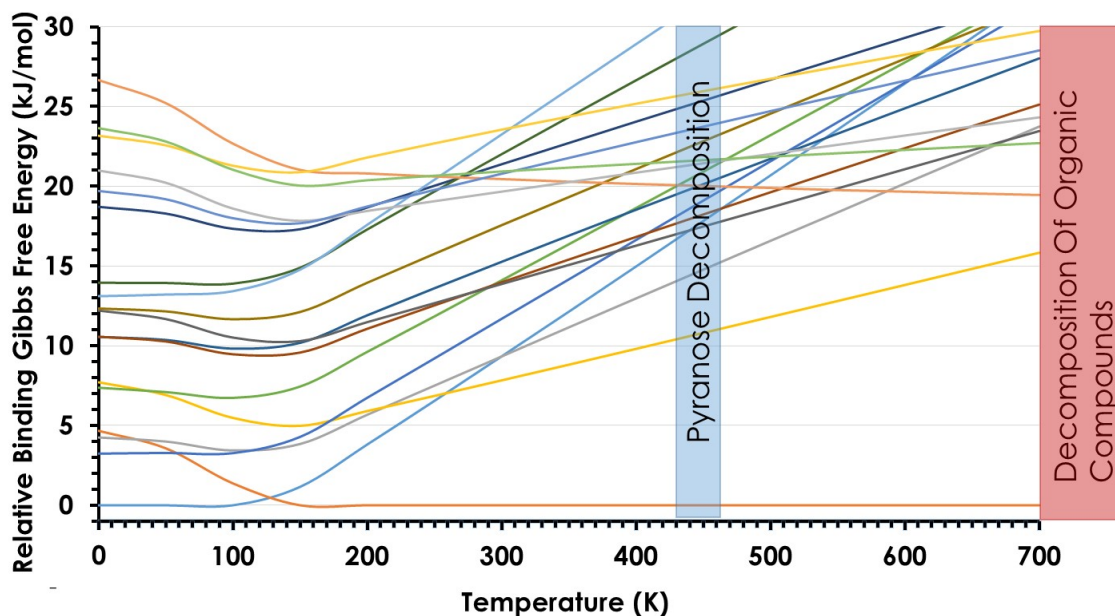


Figure S07. Gibbs relative free energy of the conformations for of β -PhGlc•Par for the structures in Figure S02. The red bar indicates the temperature at which most of the organic compounds decompose, while the blue bar indicates the temperature of decomposition of pyranose. The orange bar indicates where ΔG becomes positive and therefore, the cluster is no longer stable.



Structure of β -PhGlc • Par:

- 1 — 2 — 3 — 4 — 5 — 6 — 7 — 8 — 9
 — 10 — 11 — 12 — 13 — 14 — 15 — 16 — 17 — 18

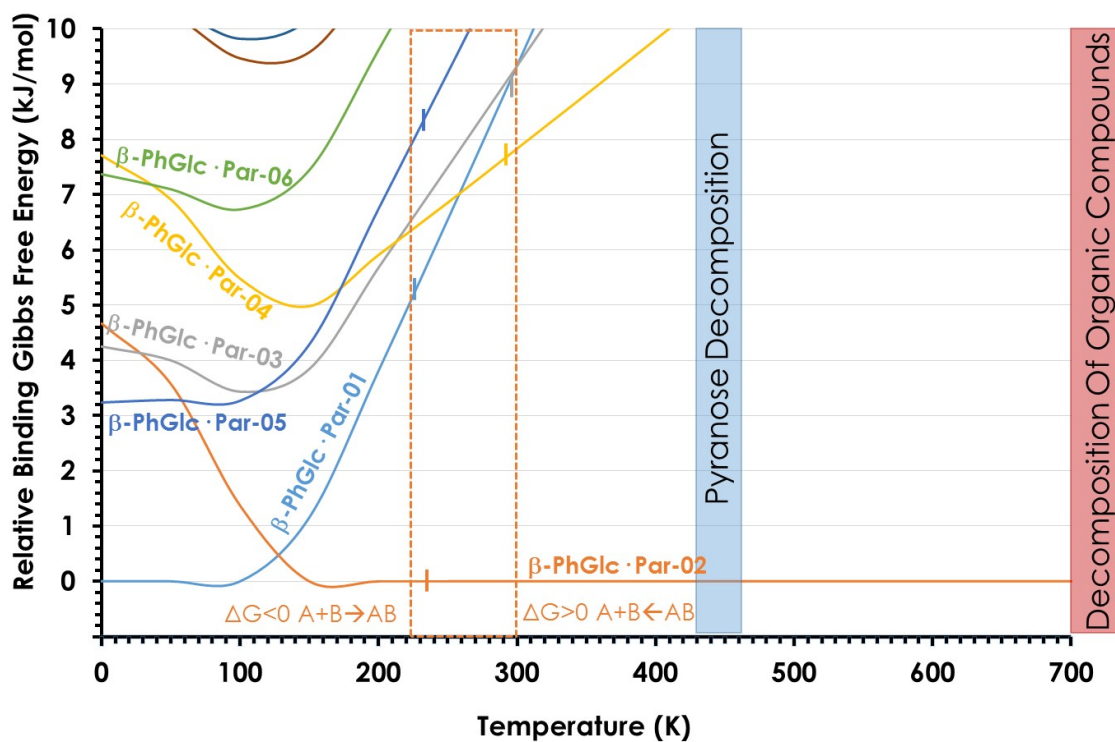
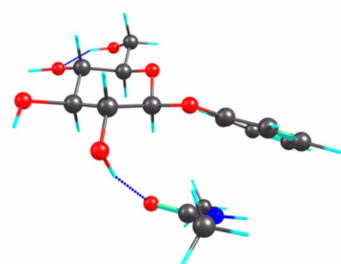
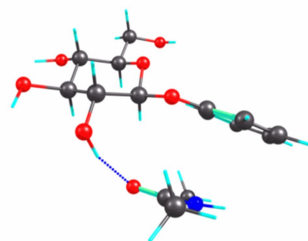


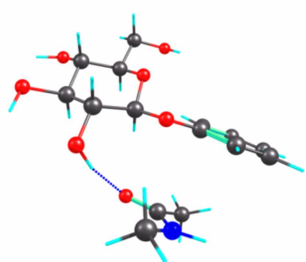
Figure S08. Calculated structures for mAct• β -PhGlc at M06-2X/6-311++G(d,p) level arranged in energetically order respect to the global minimum. Adapted from reference⁷



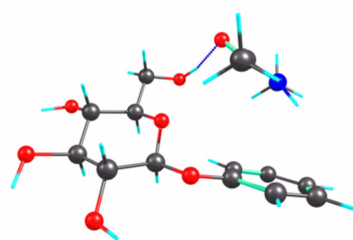
β -PhGlc · mAct-01



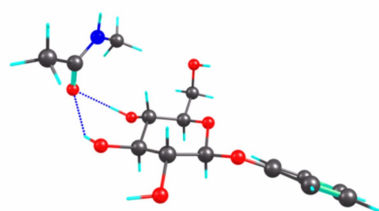
β -PhGlc · mAct-02



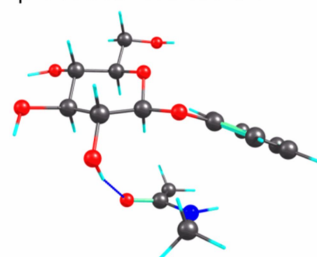
β -PhGlc · mAct-03



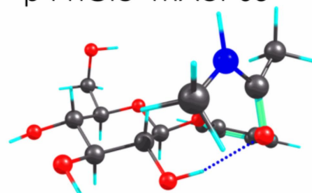
β -PhGlc · mAct-04



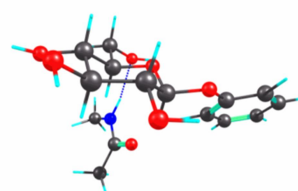
β -PhGlc · mAct-05



β -PhGlc · mAct-06

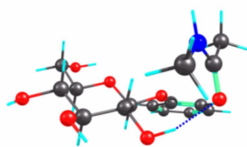


β -PhGlc · mAct-07

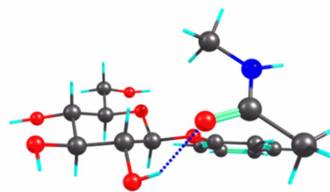


β -PhGlc · mAct-08

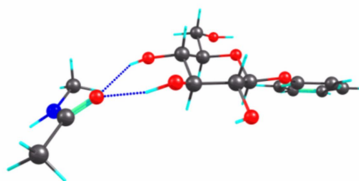
Figure S08. Cont.



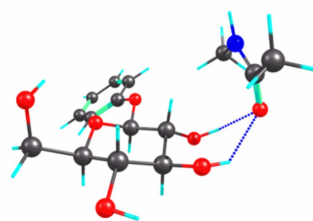
β -PhGlc · mAct-09



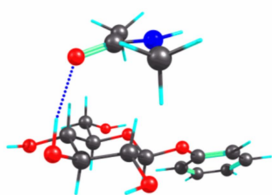
β -PhGlc · mAct-10



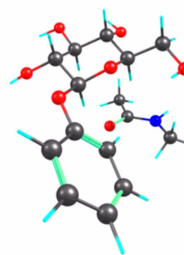
β -PhGlc · mAct-11



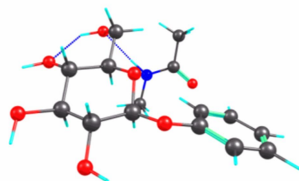
β -PhGlc · mAct-12



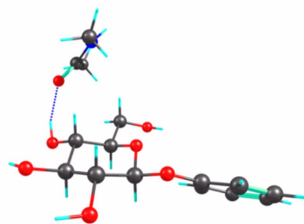
β -PhGlc · mAct-13



β -PhGlc · mAct-14

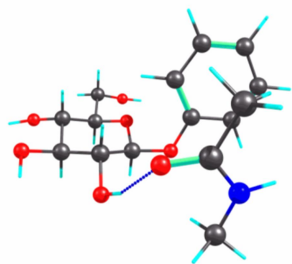


β -PhGlc · mAct-15

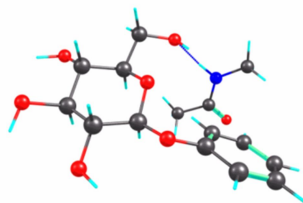


β -PhGlc · mAct-16

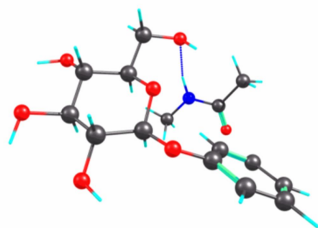
Figure S08. Cont.



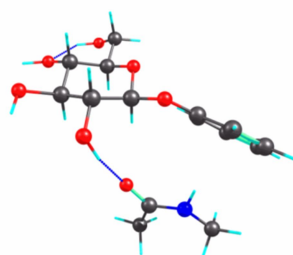
β -PhGlc · mAct-17



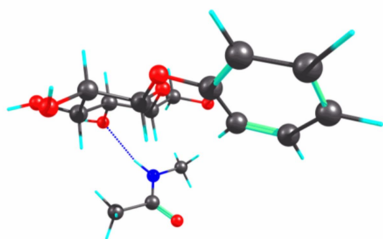
β -PhGlc · mAct-18



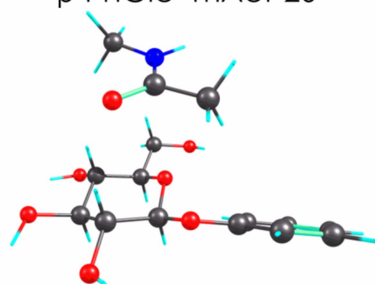
β -PhGlc · mAct-19



β -PhGlc · mAct-20



β -PhGlc · mAct-21



β -PhGlc · mAct-22

Figure S09. Calculated structures for mAct and β -PhGlc monomers at M06-2X/6-311++G(d,p) level arranged in energetically order respect to the global minimum. Adapted from reference⁷

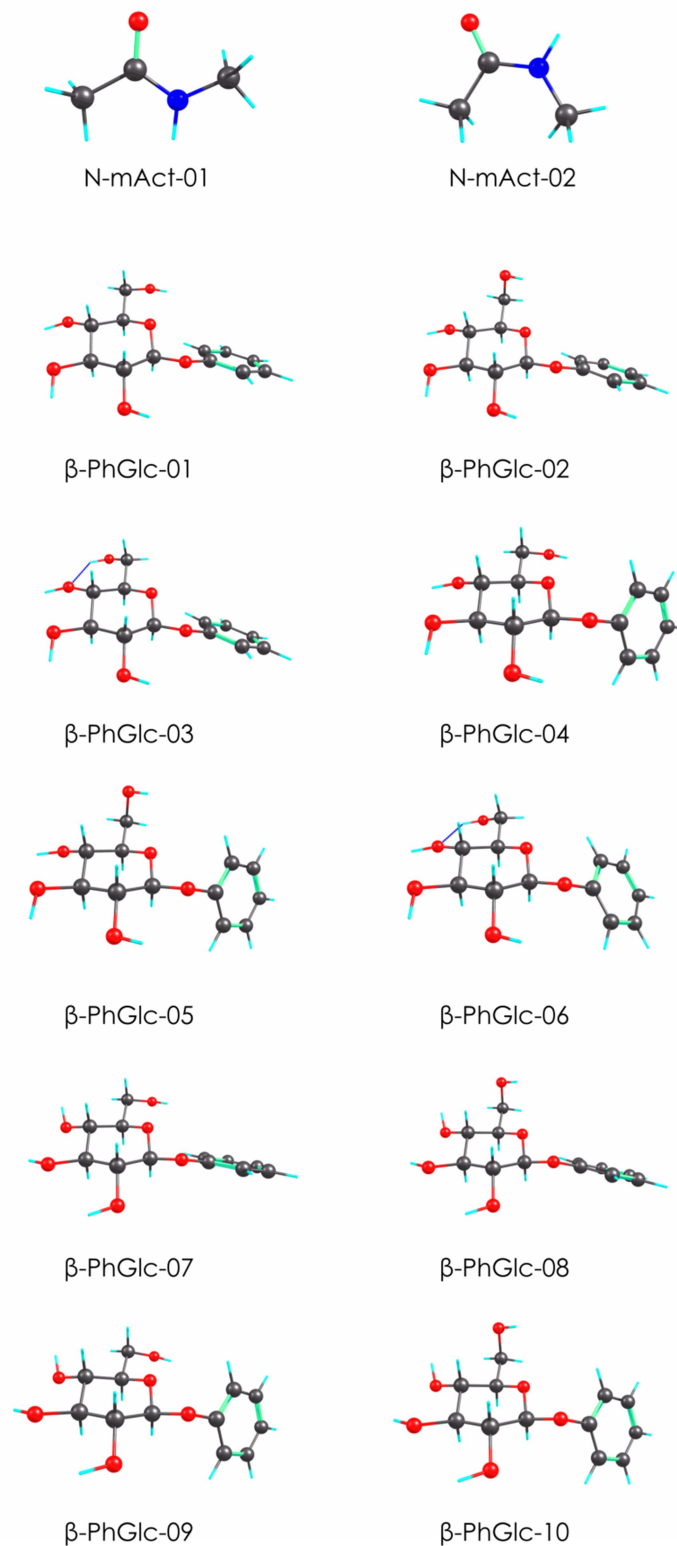


Table S04. Energies, ZPE, BSSE, thermal corrections, relative energies, sum of electronic and thermal free energies at 298.15 K (ΔG), and the equilibrium temperature calculated at M06-2X/6-311++G(d,p) level for the mAct• β -PhGlc. Adapted from reference⁷

Structure	Energy (Hartree)	ZPE (Hartree)	BSSE (Hartree)	Thermal Correction (Hartree)	Relative Energy (kJ/mol)	Relative Gibbs Free Energy (kJ/mol)	Equilibrium Temperature(K)
β -PhGlc·mAct-1	-1166.659012	0.387328	0.0025429	0.334014	1.01	0.00	257.6
β -PhGlc·mAct-2	-1166.66023	0.388116	0.0025868	0.335947	0.00	1.88	250.3
β -PhGlc·mAct-3	-1166.658745	0.387539	0.0025876	0.33498	2.39	3.24	242.4
β -PhGlc·mAct-4	-1166.658122	0.387425	0.0026193	0.334614	3.81	3.91	237.7
β -PhGlc·mAct-5	-1166.654933	0.386865	0.0020097	0.331464	9.11	4.01	237.5
β -PhGlc·mAct-6	-1166.659098	0.388665	0.0026451	0.336132	4.57	5.34	232.1
β -PhGlc·mAct-7	-1166.654346	0.38665	0.0020734	0.331818	10.25	6.48	224.2
β -PhGlc·mAct-8	-1166.652053	0.387038	0.002045	0.330148	17.22	8.12	204.8
β -PhGlc·mAct-9	-1166.654058	0.386738	0.0020318	0.332191	11.13	8.22	216.3
β -PhGlc·mAct-10	-1166.65441	0.387221	0.0021562	0.332689	11.80	8.60	212.6
β -PhGlc·mAct-11	-1166.651872	0.387322	0.0013796	0.330815	16.69	10.35	204.6
β -PhGlc·mAct-12	-1166.652939	0.387024	0.0019942	0.33194	14.72	10.50	201.8
β -PhGlc·mAct-13	-1166.650993	0.386461	0.0021083	0.33016	18.65	10.94	189.9
β -PhGlc·mAct-14	-1166.650403	0.386606	0.0019432	0.33065	20.15	13.77	176.6
β -PhGlc·mAct-15	-1166.651961	0.387133	0.0018169	0.332573	17.11	14.73	183.9
β -PhGlc·mAct-16	-1166.650015	0.386881	0.0014999	0.330815	20.72	15.22	175.7
β -PhGlc·mAct-17	-1166.652754	0.387338	0.0025232	0.333814	17.42	15.91	174.6
β -PhGlc·mAct-18	-1166.649871	0.386562	0.0015352	0.33109	20.36	16.32	164.1
β -PhGlc·mAct-19	-1166.651372	0.387065	0.0017518	0.332672	18.30	16.54	178.3
β -PhGlc·mAct-20	-1166.651388	0.387738	0.0021485	0.333154	21.07	17.76	145.1
β -PhGlc·mAct-21	-1166.647822	0.386426	0.0017138	0.330232	25.85	19.45	143.7
β -PhGlc·mAct-22	-1166.648724	0.38607	0.0023895	0.331251	24.32	19.76	172.1

Table S05. Energies, ZPE, thermal corrections, relative energies and the sum of electronic and thermal free energies at 298.15 K (ΔG) calculated at M06-2X/6-311++G(d,p) level for the mAct• β -PhGlc. Adapted from reference⁷

Structure	Energy (Hartree)	ZPE (Hartree)	Thermal Correction (Hartree)	Relative Energy (kJ/mol)	Relative Gibbs Free Energy (kJ/mol)
b-PhGlc-1	-918.148769	0.281637	0.237167	0.00	0.00
b-PhGlc-2	-918.148303	0.281844	0.237559	1.77	2.25
b-PhGlc-3	-918.147723	0.282161	0.238269	4.12	5.64
b-PhGlc-5	-918.146287	0.281640	0.236675	6.52	5.22
b-PhGlc-4	-918.146551	0.281975	0.237231	6.71	5.99
b-PhGlc-6	-918.145782	0.281954	0.237133	8.67	7.75
b-PhGlc-8	-918.144428	0.281832	0.237328	11.91	11.82
b-PhGlc-7	-918.142671	0.281169	0.236572	14.78	14.45
b-PhGlc-10	-918.142498	0.281676	0.235892	16.57	13.12
b-PhGlc-9	-918.140614	0.281679	0.236713	21.52	20.22

Structure	Energy (Hartree)	ZPE (Hartree)	Thermal Correction (Hartree)	Relative Energy (kJ/mol)	Relative Gibbs Free Energy (kJ/mol)
N-mAct-01	-248.486064	0.102554	0.072236	0.00	0.00
N-mAct-02	-248.482527	0.102665	0.072858	9.58	10.92

Figure S10. IR spectra of mAct• β -PhGlc and the predicted spectra for the structures in Figure S01 calculated at M06-2X/6-311++G(d,p). A correction factor of 0.939 was employed to account for the anharmonicity. Adapted from reference⁷

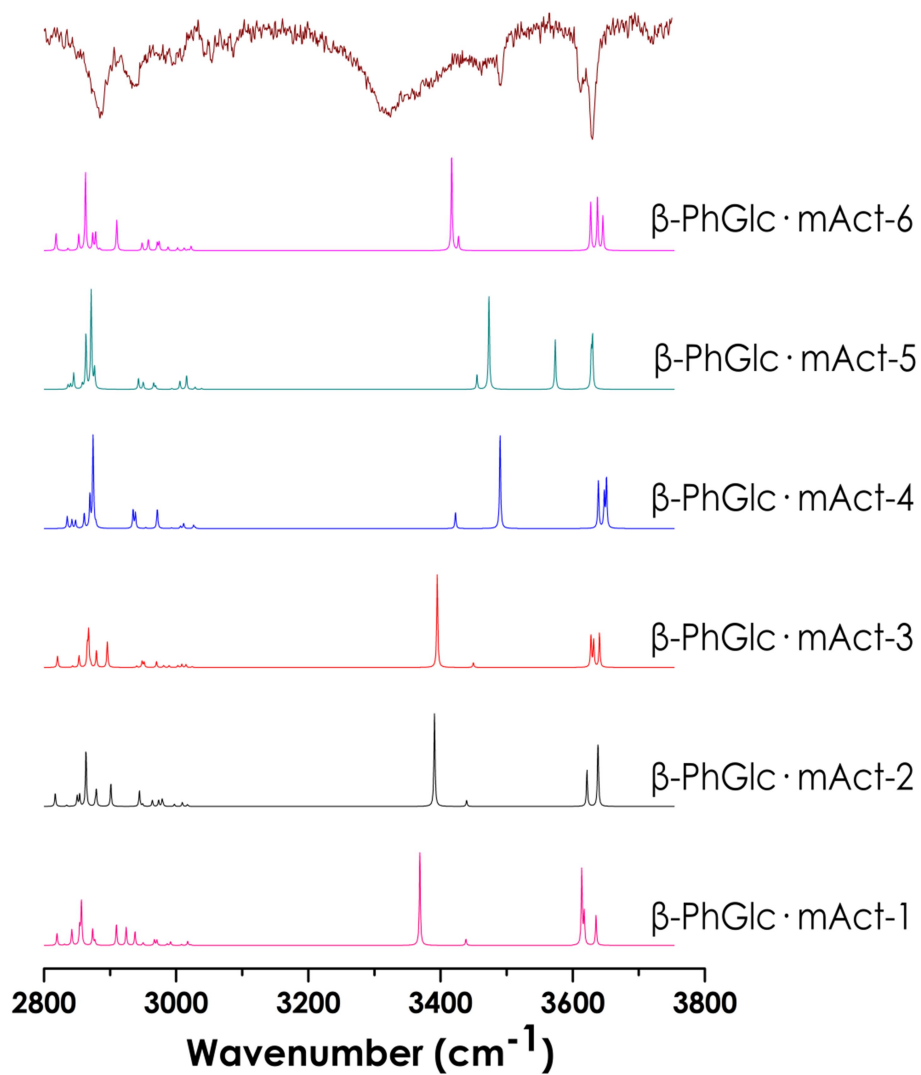


Figure S10. Cont.

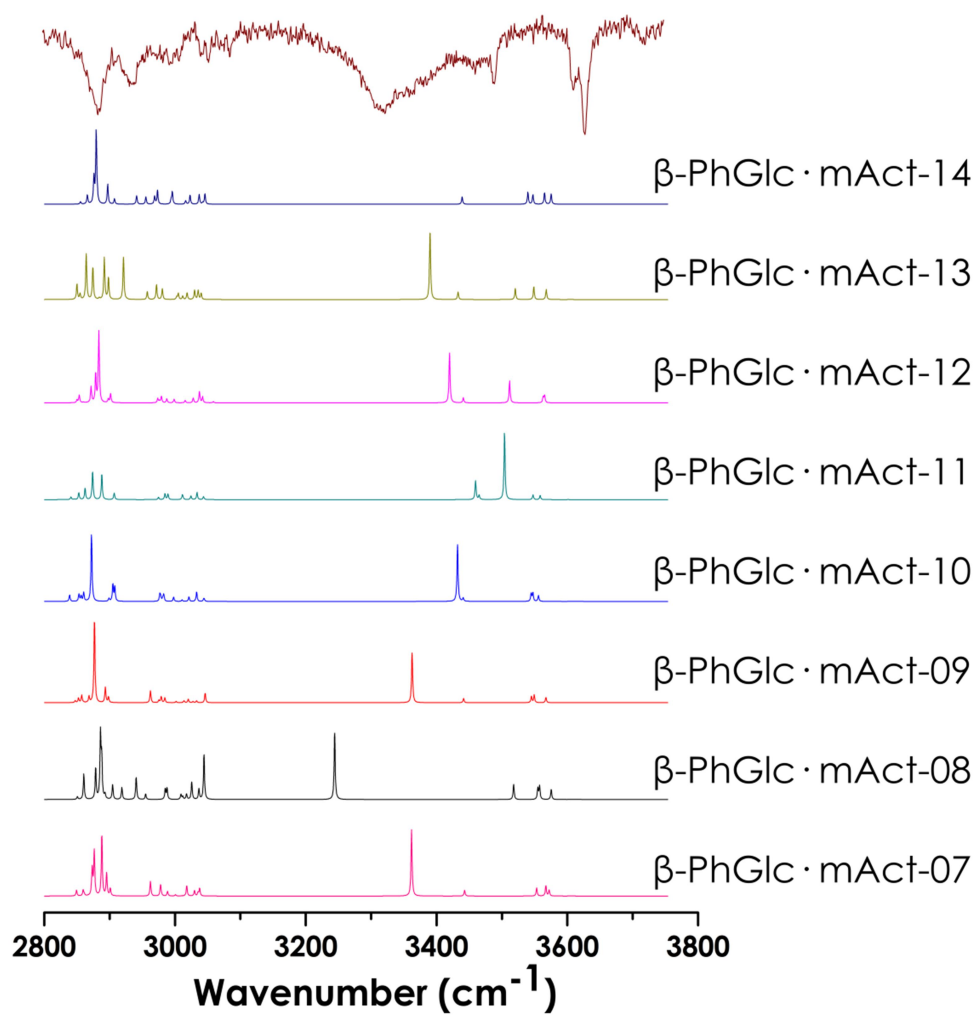


Figure S10. Cont.

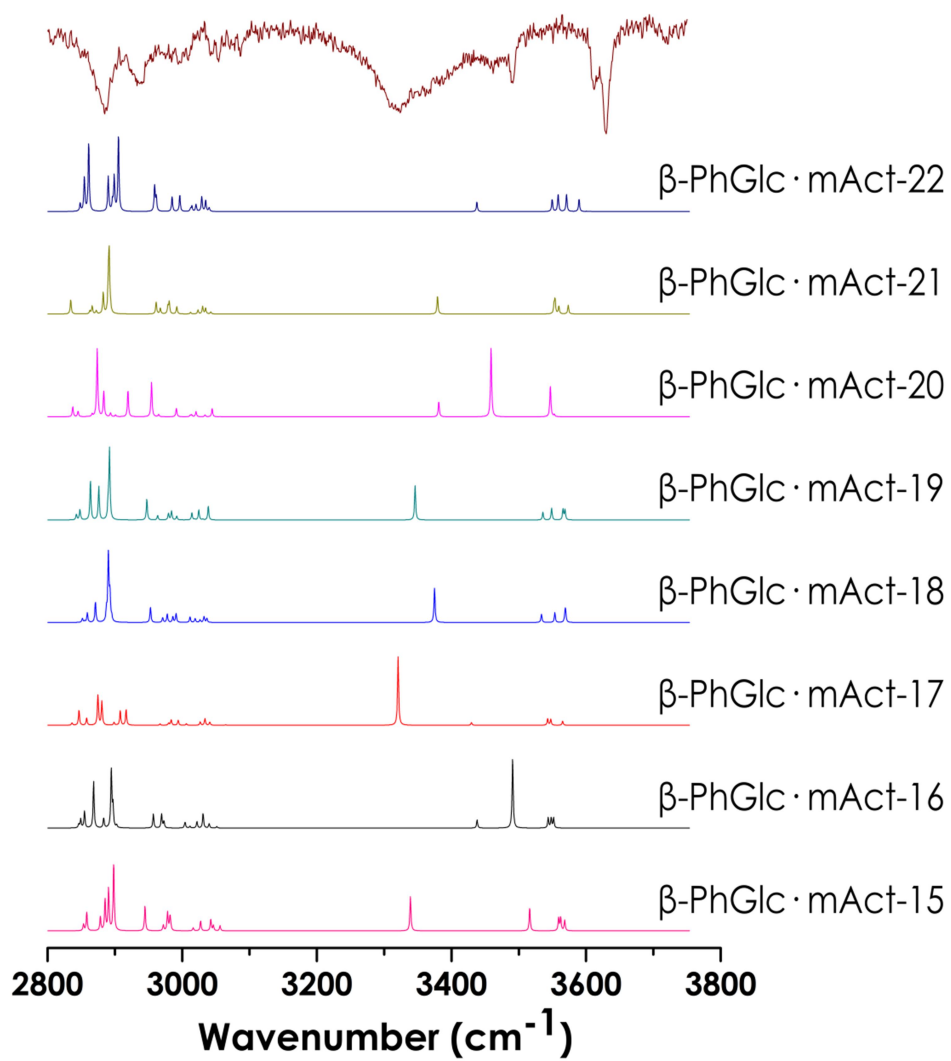


Figure S11. Gibbs relative free energy of the conformations for mAct· β -PhGlc for the structures in Figure S01. The red bar indicates the temperature at which most of the organic compounds decompose, while the blue bar indicates the temperature of decomposition of pyranose. The orange bar indicates where ΔG becomes positive and therefore, the cluster is no longer stable. Adapted from reference⁷

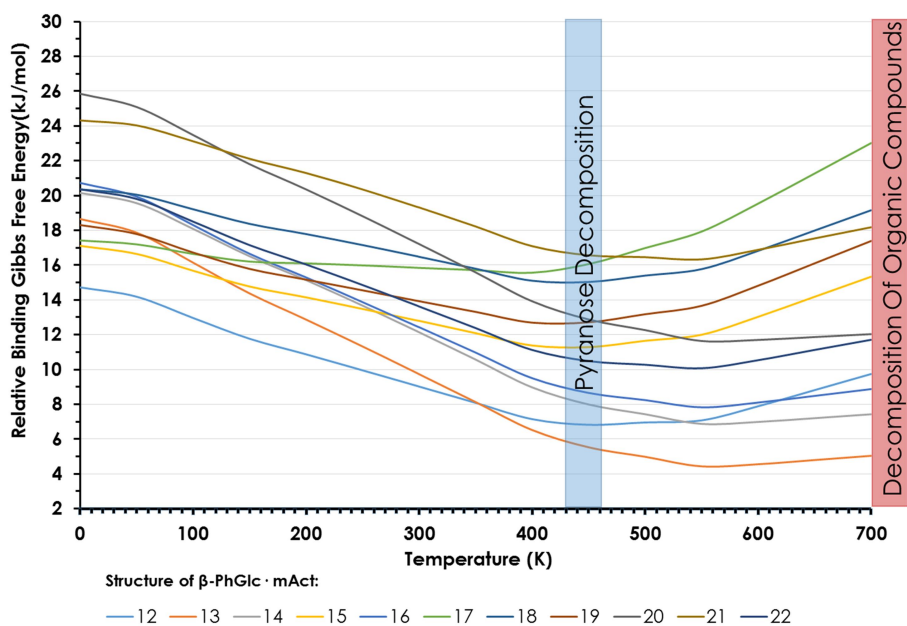
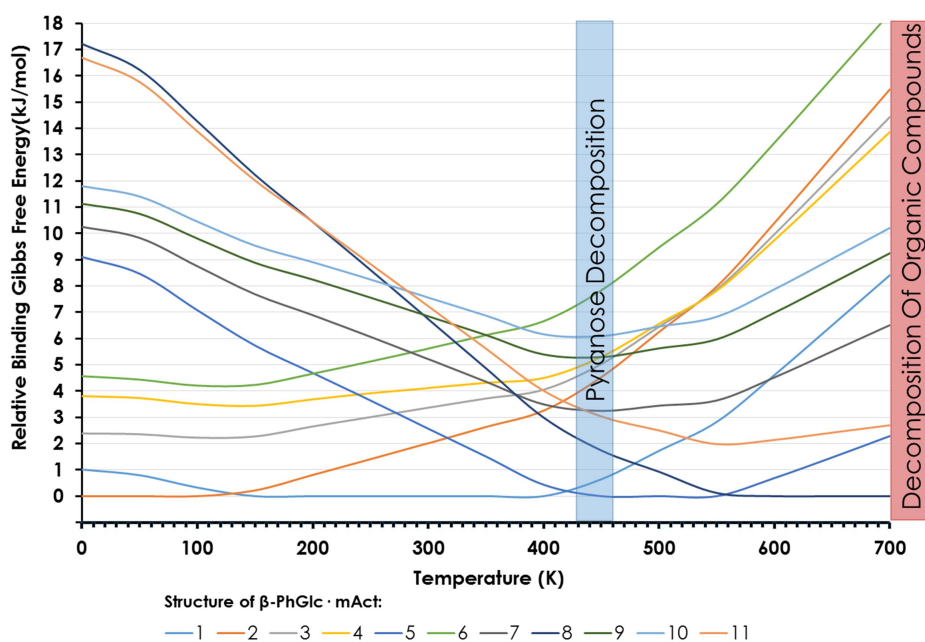
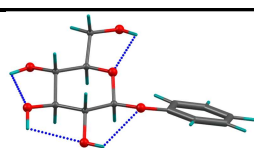
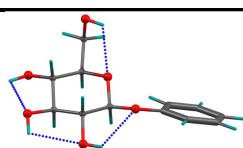


Table S06. Complete list of conformational isomers of β -PhGlc $\cdots\alpha$ -Glc in a 40 kJ/mol window, computed at the M06-2X/6-311++G(d,p) level, together with their relative stability. RE ZPE: ZPE-corrected relative stability; RE GIBBS: relative ΔG at 298 K; β -PhGlc-n/ α -Glc-n: isomer of the monomer in the complex (see structures at the bottom of the table); H BOND: description of the hydrogen bond network in the complex. Adapted from reference⁸

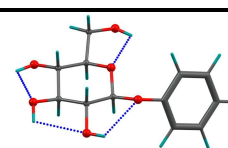
ISOMER	RE ZPE (kJ/mol)	RE GIBBS (kJ/mol)	β -PhGlc (P)	α -Glc (A)	H BOND
β -PhGlc $\cdot\alpha$ -Glc_01	0.00	0.00	β -PhGlc-1	α -Glc-4	A6P6A5-A1P5
β -PhGlc $\cdot\alpha$ -Glc_02	7.49	6.72	β -PhGlc-1	α -Glc-4	A6P4-A1P6
β -PhGlc $\cdot\alpha$ -Glc_03	8.49	8.35	β -PhGlc-2	α -Glc-4	A3P6A2
β -PhGlc $\cdot\alpha$ -Glc_04	8.58	6.46	β -PhGlc-2	α -Glc-4	P6A6-P4A1P3
β -PhGlc $\cdot\alpha$ -Glc_05	8.81	11.85	β -PhGlc-1	α -Glc-3	A6P6A5
β -PhGlc $\cdot\alpha$ -Glc_06	12.07	9.50	β -PhGlc-2	α -Glc-4	P6A2P5
β -PhGlc $\cdot\alpha$ -Glc_07	12.33	14.11	β -PhGlc-1	α -Glc-4	A6P6A5-A1P5
β -PhGlc $\cdot\alpha$ -Glc_08	18.60	14.86	β -PhGlc-1	α -Glc-4	P6A2
β -PhGlc $\cdot\alpha$ -Glc_09	18.69	18.21	β -PhGlc-1	α -Glc-4	P6A2
β -PhGlc $\cdot\alpha$ -Glc_10	18.77	18.08	β -PhGlc-1	α -Glc-3	A6P5
β -PhGlc $\cdot\alpha$ -Glc_11	20.01	20.39	β -PhGlc-2	α -Glc-4	A2P6A1
β -PhGlc $\cdot\alpha$ -Glc_12	20.35	21.30	β -PhGlc-1	Boat Structure	A6P6A5-A1P5
β -PhGlc $\cdot\alpha$ -Glc_13	20.36	21.31	β -PhGlc-1	Boat Structure	A6P6A5-A1P5
β -PhGlc $\cdot\alpha$ -Glc_14	20.56	20.54	β -PhGlc-1	α -Glc-4	P6A6P5
β -PhGlc $\cdot\alpha$ -Glc_15	21.56	21.43	β -PhGlc-2	α -Glc-3	A2P6A1
β -PhGlc $\cdot\alpha$ -Glc_16	22.17	24.64	β -PhGlc-2	α -Glc-4	A2P5-P6A1
β -PhGlc $\cdot\alpha$ -Glc_17	26.56	23.67	β -PhGlc-4	α -Glc-4	P6A2
β -PhGlc $\cdot\alpha$ -Glc_18	35.63	36.91	β -PhGlc-1	Boat Structure	A6P6A5
β -PhGlc $\cdot\alpha$ -Glc_19	36.35	36.72	β -PhGlc-4	Boat Structure	A1P6A6
β -PhGlc $\cdot\alpha$ -Glc_20	38.20	40.87	β -PhGlc-2	Boat Structure	A6P5-P6A4
β -PhGlc $\cdot\alpha$ -Glc_21	38.34	38.93	β -PhGlc-2	Boat Structure	P6A5-A1P5



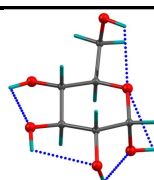
β -PhGlc-1



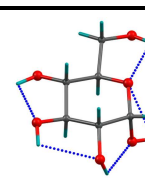
β -PhGlc-2



β -PhGlc-4



α -Glc-3



α -Glc-4

Figure S12. Relative Gibbs binding free energy of some selected isomers of β -PhGlc $\cdots\alpha$ -Glc. The triangles highlight the temperature at which $\Delta G = 0$ for each isomer. The colour code matches that in [Figures S13](#) and [S16](#). Adapted from reference⁸

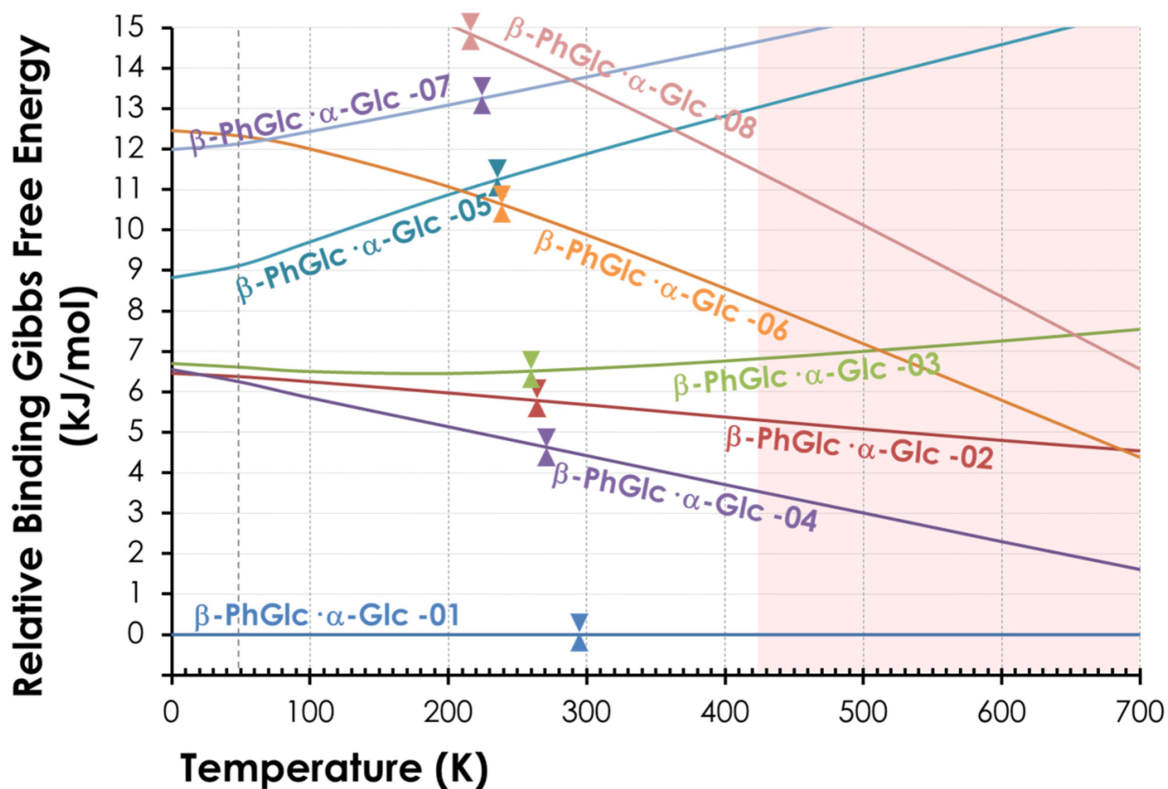


Figure S13. Most stable conformers of β -PhGlc \cdots α -Glc in a ~ 10 kJ/mol energy window. The hydroxymethyl groups (blue and red lines identify different isomers) and the anomeric carbon (highlighted with a green circle) of each monomer are evidenced in order to help the reader to follow the structural changes (arrows). Adapted from reference⁸

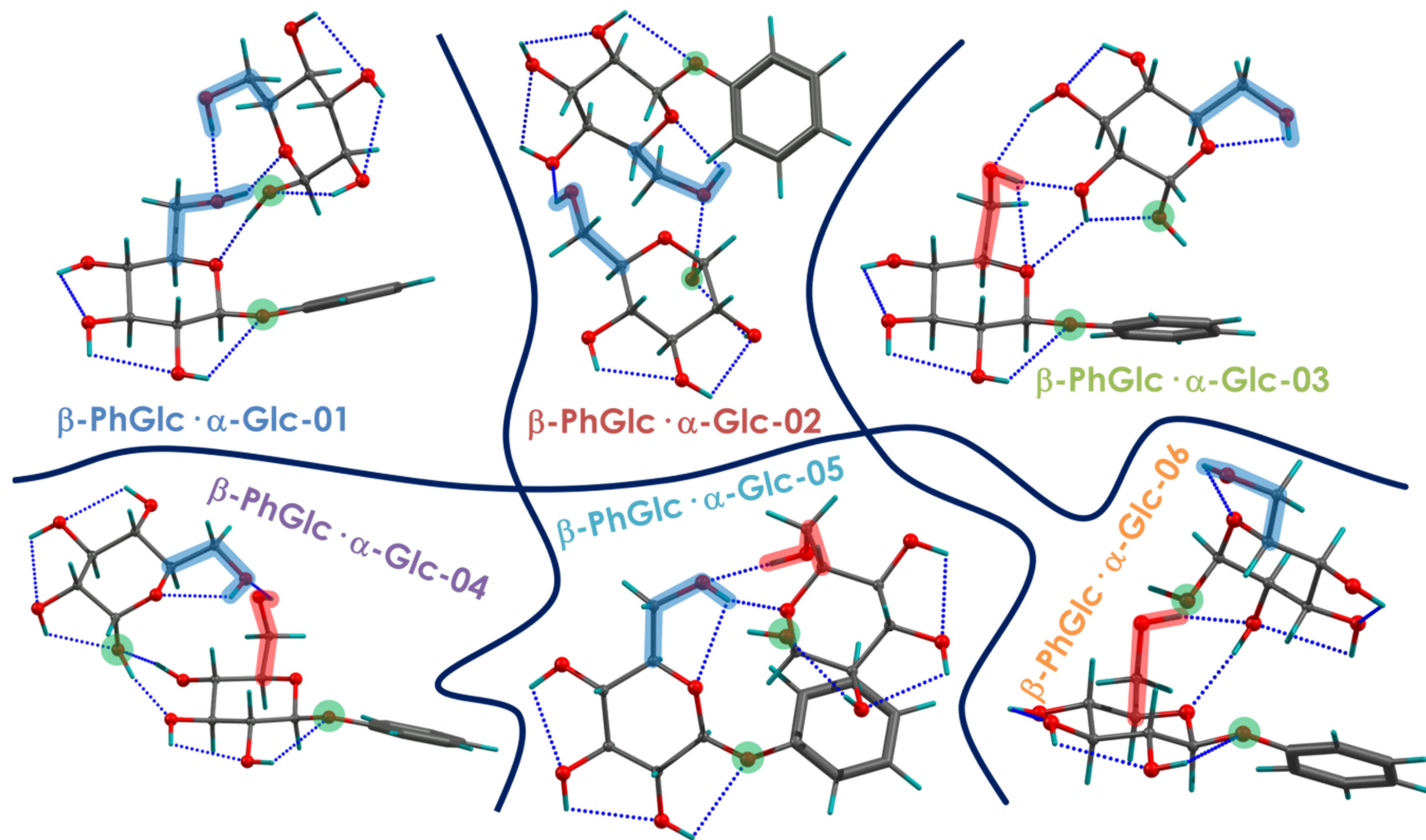


Table S07. Complete list of conformational isomers of β -PhGlc \cdots β -Glc in a 35 kJ/mol window, computed at the M06-2X/6-311++G(d,p) level, together with their relative stability. RE ZPE: ZPE-corrected relative stability; RE GIBBS: relative ΔG at 298 K; β -PhGlc-n/ β -MeGlc-n: isomer of the monomer in the complex (see structures at the bottom of the table); H BOND: description of the hydrogen bond network in the complex. Adapted from reference⁸

ISOMER	RE ZPE (kJ/mol)	RE GIBBS (kJ/mol)	β -PhGlc (P)	β -Glc (B)	H BOND
β -PhGlc \cdot β -Glc_01	0.00	0.00	β -PhGlc-2	β -Glc-3	B2P6B1P5-P2B6P1
β -PhGlc \cdot β -Glc_02	0.79	0.38	β -PhGlc-5	β -Glc-3	B2P6B1P5-P2B6P1
β -PhGlc \cdot β -Glc_03	12.10	10.43	β -PhGlc-2	β -Glc-4	P6B1P5-P2B6P1
β -PhGlc \cdot β -Glc_04	13.24	10.46	β -PhGlc-1	β -Glc-3	B2P6B1-P2B6P1
β -PhGlc \cdot β -Glc_05	14.36	6.26	β -PhGlc-1	β -Glc-4	B6P6-B1P4
β -PhGlc \cdot β -Glc_06	15.29	10.56	β -PhGlc-1	β -Glc-2	B1P4-P3B6P2
β -PhGlc \cdot β -Glc_07	16.90	15.45	β -PhGlc-2	β -Glc-4	B2P6B1P5-P2B6P1
β -PhGlc \cdot β -Glc_08	18.21	10.98	β -PhGlc-2	β -Glc-3	B4P2B3
β -PhGlc \cdot β -Glc_09	20.75	6.50	β -PhGlc-1	β -Glc-4	B6P4B5-P1B3
β -PhGlc \cdot β -Glc_10	22.14	16.85	β -PhGlc-5	β -Glc-4	P6B1P5-P2B6
β -PhGlc \cdot β -Glc_11	23.41	15.49	β -PhGlc-1	β -Glc-4	B6P4B5-P1B3
β -PhGlc \cdot β -Glc_12	24.64	14.95	β -PhGlc-4	β -Glc-4	B1P2B5-B6P1
β -PhGlc \cdot β -Glc_13	24.77	19.59	β -PhGlc-1	β -Glc-4	B2P2B1
β -PhGlc \cdot β -Glc_14	26.14	21.03	β -PhGlc-2	β -Glc-4	B3P6B2P5
β -PhGlc \cdot β -Glc_15	26.39	21.11	β -PhGlc-2	β -Glc-4	B3P6B2
β -PhGlc \cdot β -Glc_16	26.45	15.89	β -PhGlc-2	β -Glc-4	P4B6P3-B1P6
β -PhGlc \cdot β -Glc_17	26.88	19.22	β -PhGlc-1	β -Glc-4	B3P5-P6B2
β -PhGlc \cdot β -Glc_18	34.77	30.93	β -PhGlc-1	β -Glc-4	B2P6B3
β -PhGlc \cdot β -Glc_19	36.69	33.91	β -PhGlc-1-4	β -Glc-4	B2P6B3P5

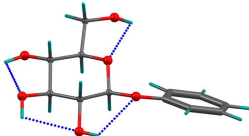
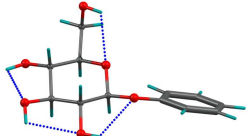
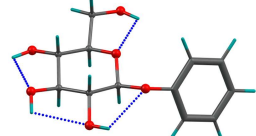
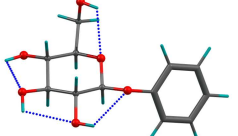
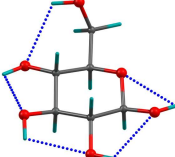
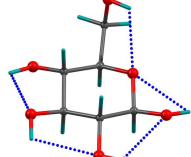
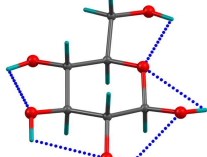
			
β -PhGlc-1	β -PhGlc-2	β -PhGlc-4	β -PhGlc-5
			
β -Glc-2	β -Glc-3	β -Glc-4	

Figure S14. Relative Gibbs binding free energy of some selected isomers of β -PhGlc $\cdots\beta$ -Glc. The triangles highlight the temperature at which $\Delta G = 0$ for each isomer. The colour code matches that in [Figures S15](#) and [S16](#). Adapted from reference⁸

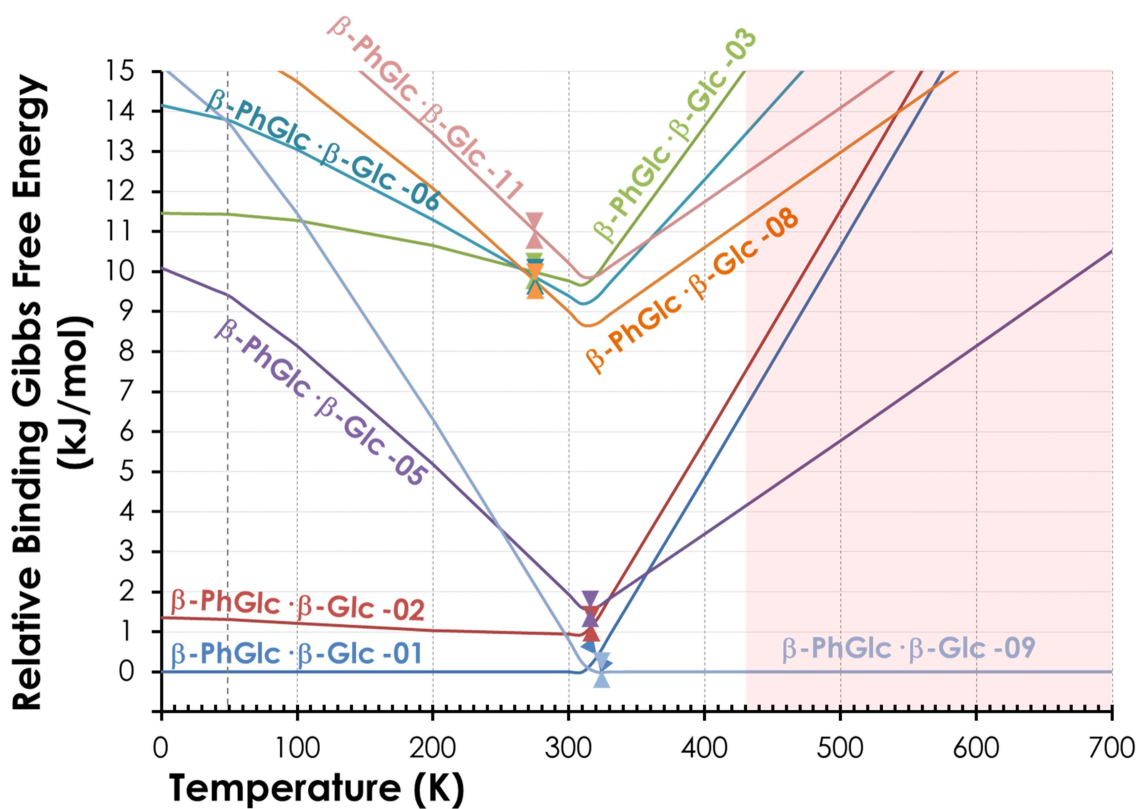


Figure S15. Most stable conformers of β -PhGlc \cdots β -Glc in a ~ 10 kJ/mol energy window. The hydroxymethyl groups (blue and red lines identify different isomers) and the anomeric carbon (highlighted with a green circle) of each monomer are evidenced in order to help the reader to follow the structural changes (arrows). Adapted from reference⁸

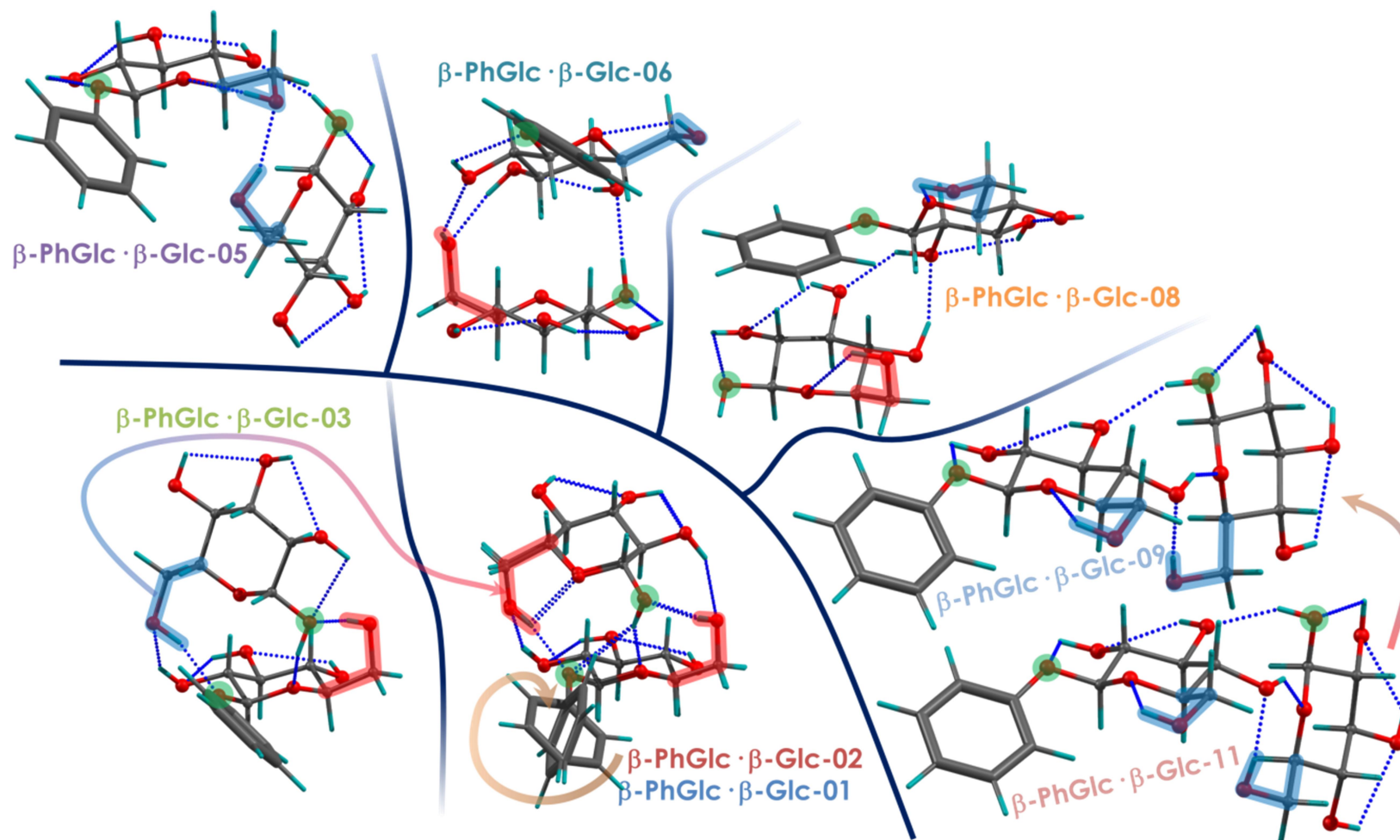


Figure S16. Comparison between the IR/UV of β -PhGlc \cdots Glc recorded probing at 36900 cm^{-1} and the simulated spectra for some selected calculated structures of β -PhGlc $\cdots\alpha$ -Glc (upper panel) and β -PhGlc $\cdots\beta$ -Glc (lower panel). A correction factor of 0.9385 in the OH stretching region and of 0.9525 in the CH stretching region was used to account for the anharmonicity. The colour code matches that of [Figures S12, S13, S14](#) and [S15](#). Adapted from reference⁸

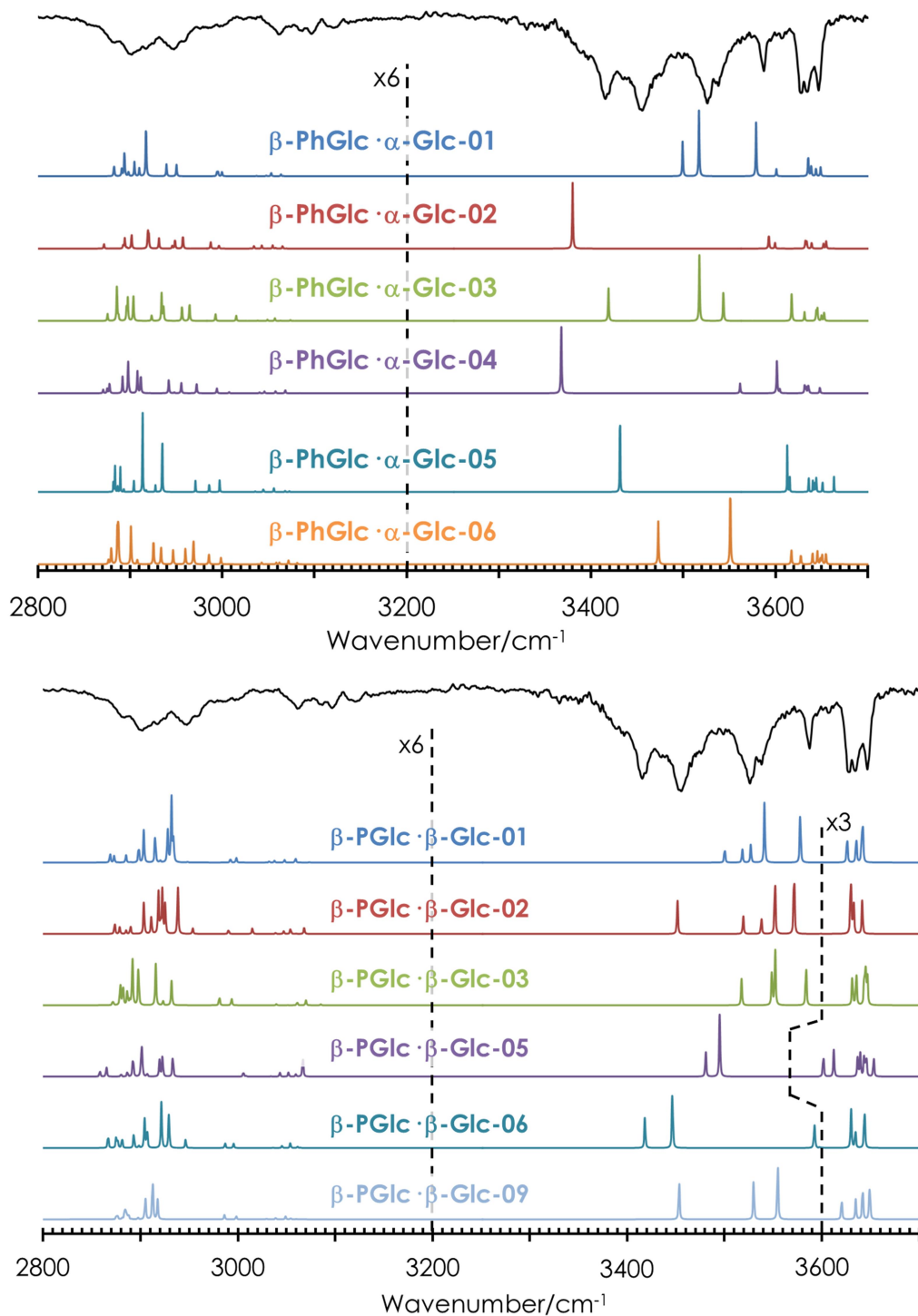


Figure S17. Five lowest energy structures of methyl- α -D-Glucopyranose...Phenol calculated at M062x/6-311++G(d,p) level. Relative stability in kJ/mol. Adapted from reference¹

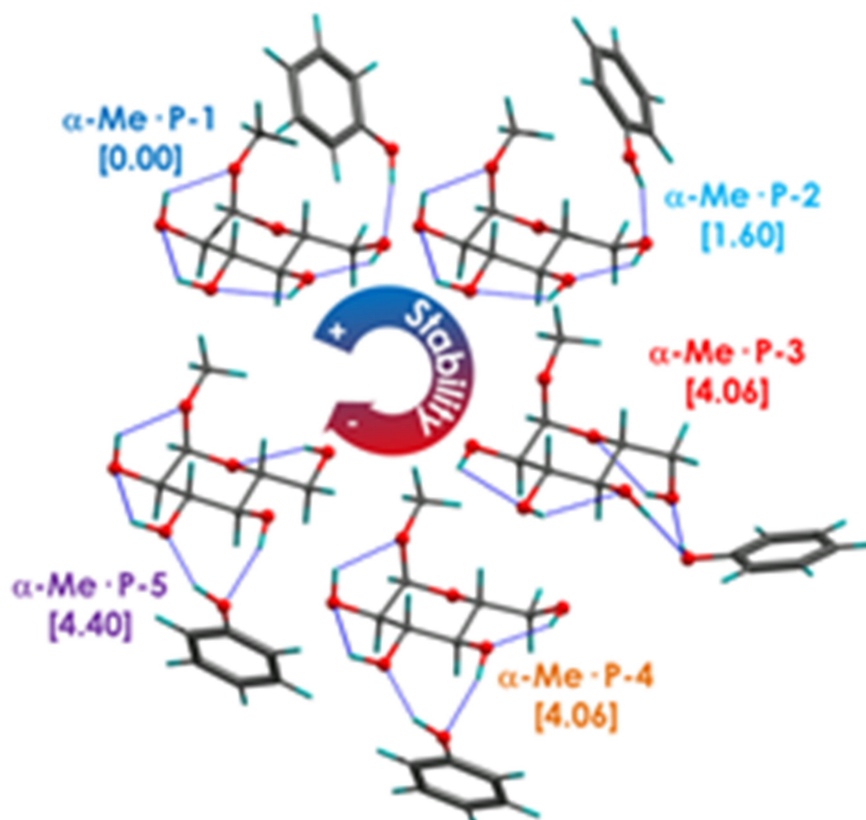


Figure S18. Comparison between experimental IR/UV spectra and simulated ones for methyl- α -D-Glucopyranose...Phenol. The same spectrum was obtained with the UV laser at 36539 and 36714 cm^{-1} , while the lower trace was obtained probing at 36335 cm^{-1} . The resulting spectrum from subtracting both traces is also shown for comparison. Adapted from reference¹

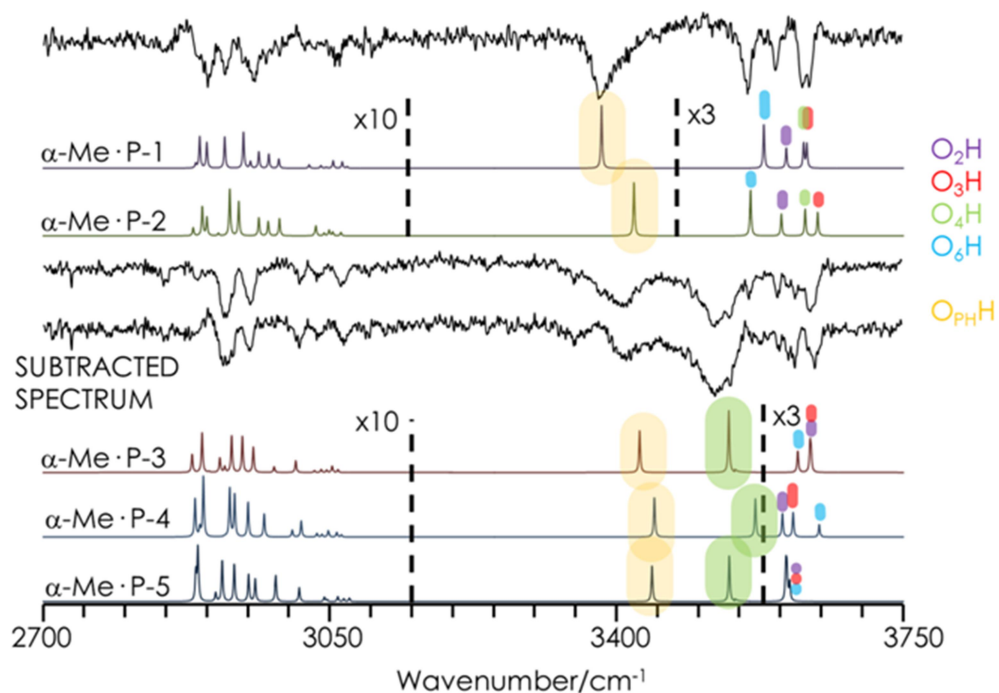


Figure S19. Seven lowest energy structures of methyl- β -D-Glucopyranose...Phenol calculated at M06-2X/6-311++G(d,p) level. Relative stability in kJ/mol. Adapted from reference¹

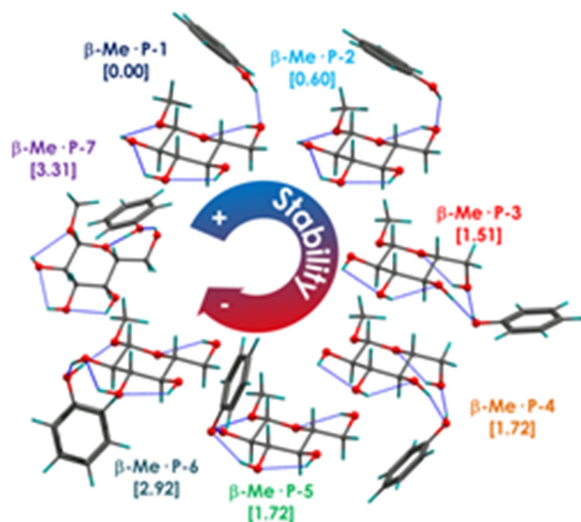


Figure S20. Comparison between experimental IR/UV spectra and simulated ones for methyl- β -D-Glucopyranose...Phenol. Adapted from reference¹

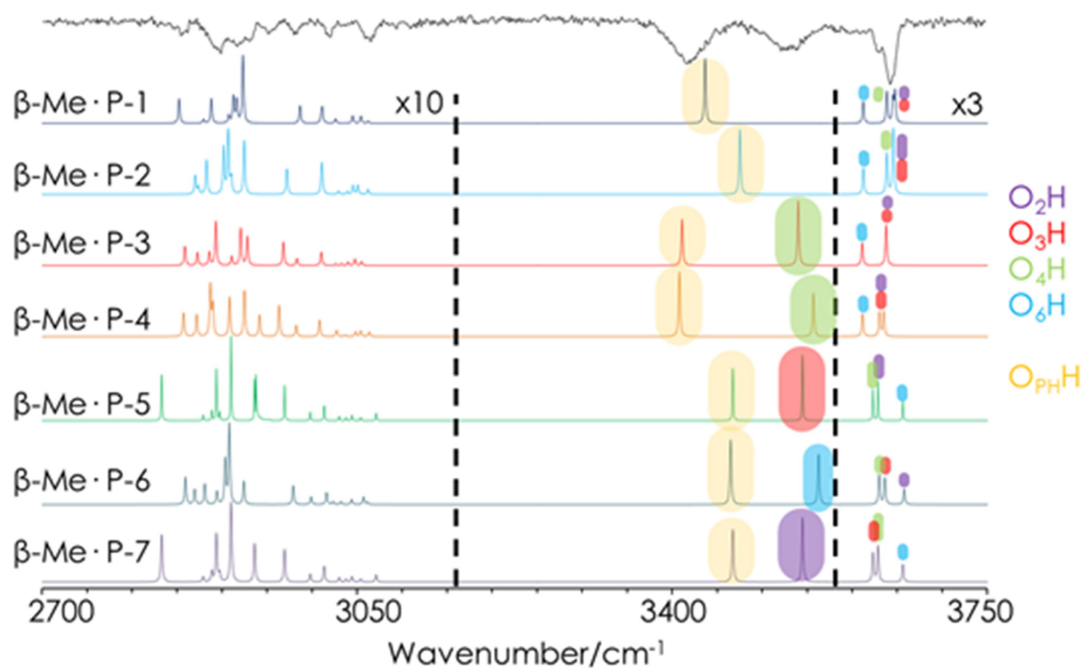


Figure S21. Five lowest energy structures of phenyl- β -D-Glucopyranose...Phenol calculated at M06-2X/6-311++G(d,p) level. Relative stability in kJ/mol. Adapted from reference¹

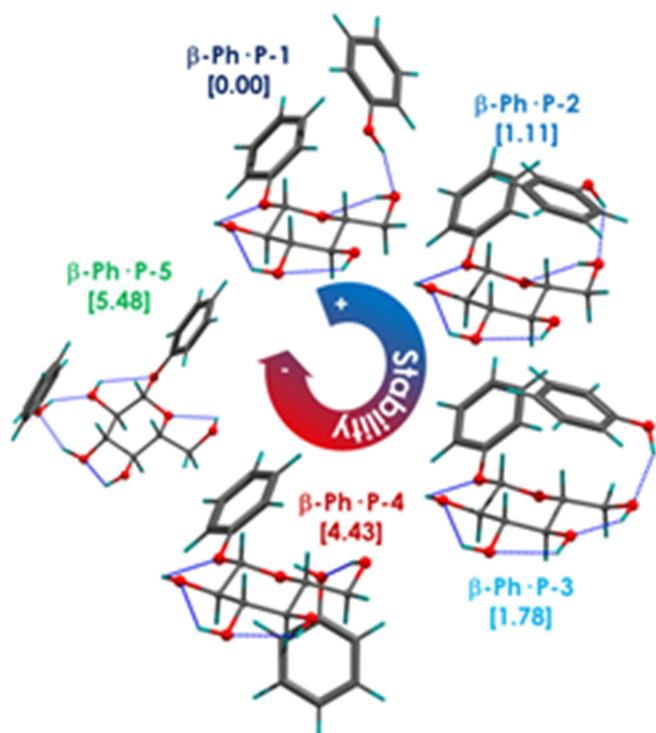


Figure S22. Comparison between experimental IR/UV spectra and simulated ones for phenyl- α -D-Glucopyranose...Phenol. Adapted from reference¹

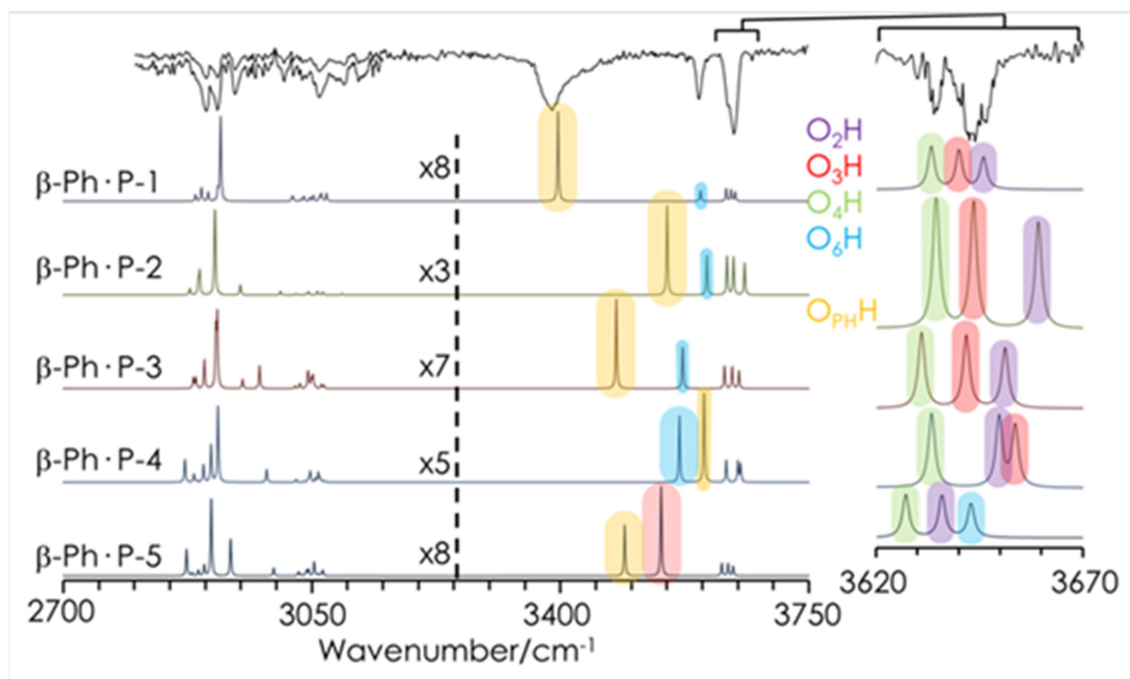
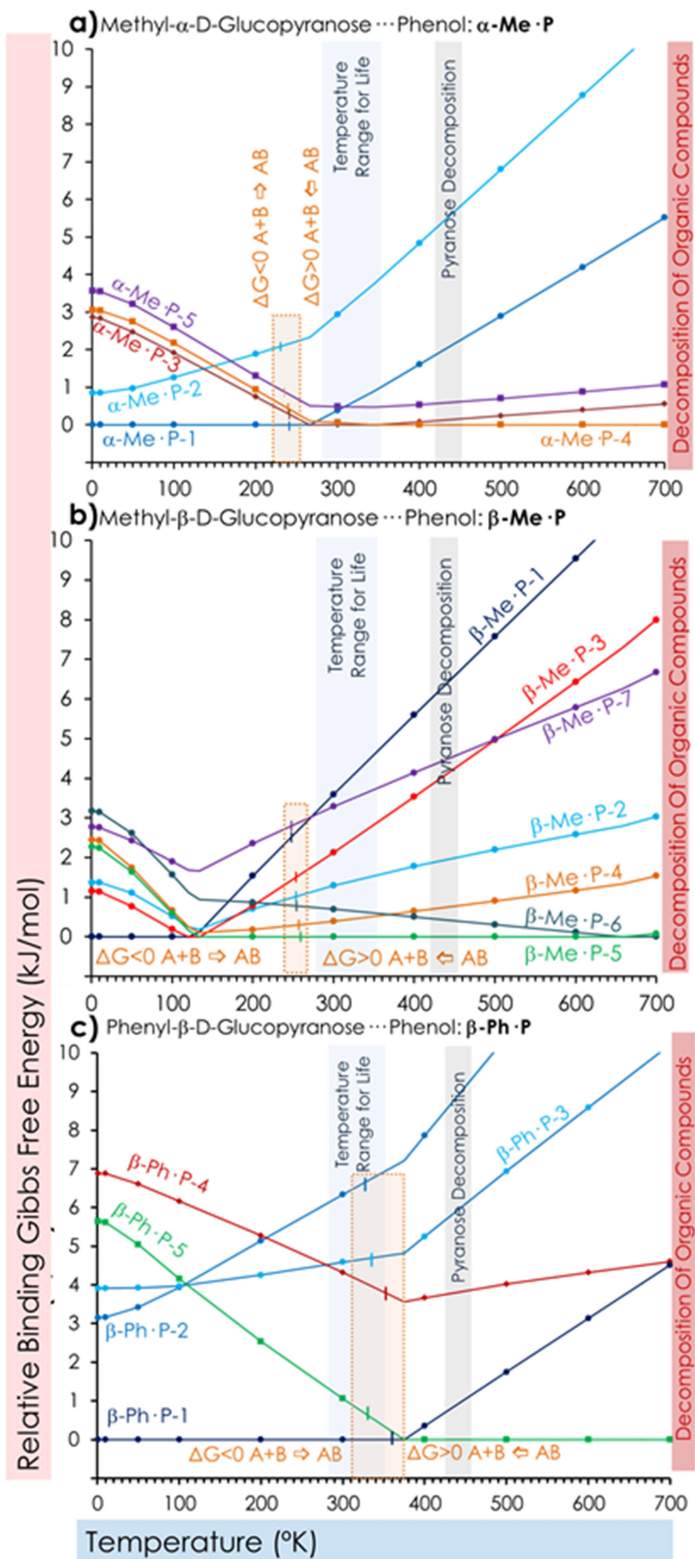


Figure S23. Gibbs relative free energy of the conformations in Figures 3, 5 and 7 for α -Me-P (a), β -Me-P (b) and β -Ph-P (c). The red bar indicates the temperature at which most of the organic compounds decompose, while the gray bar indicates the temperature of decomposition of pyranose. The pink bar indicates where ΔG becomes positive and therefore, the cluster is no longer stable. Adapted from reference¹



REFERENCES:

- 1 I. Usabiaga, J. González, P. F. Arnáiz, I. León, E. J. Cocinero and J. A. Fernández, *Phys. Chem. Chem. Phys.*, 2016, **18**, 12457–12465.
- 2 I. León, J. Millán, E. J. Cocinero, A. Lesarri and J. A. Fernández, *Angew. Chemie - Int. Ed.*, 2013, **52**, 7772–7775.
- 3 I. León, J. Millán, E. J. Cocinero, A. Lesarri and J. A. Fernández, *Angew. Chemie - Int. Ed.*, 2014, **53**, 12480–12483.
- 4 I. León, R. Montero, A. Longarte and J. a Fernández, *Phys. Chem. Chem. Phys.*, 2015, **17**, 2241–5.
- 5 I. M. Frisch, et al. Gaussian 09, Rev. A02. 2009. Wallingford CT, Gaussian, .
- 6 S. F. Boys and F. Bernardi, *Mol. Phys.*, 1970, **19**, 553–566.
- 7 A. Camiruaga, I. Usabiaga, A. Insausti, I. León and J. A. Fernández, *Phys. Chem. Chem. Phys.*, 2017, **19**, 12013–12021.
- 8 I. Usabiaga, J. González, I. León, P. F. Arnaiz, E. J. Cocinero and J. A. Fernández, *J. Phys. Chem. Lett.*, 2017, **8**, 1147–1151.